Cranial osteology of the Middle Jurassic (Callovian) *Martillichthys renwickae* (Neopterygii: Pachycormiformes), with comments on the evolution and ecology of edentulous pachycormiforms

Claire Dobson[1], Sam Giles[1,2], Zerina Johanson[3], Jeff Liston[4,5,6,7] and Matt Friedman[1,8]

[1]Department of Earth Sciences, University of Oxford, Oxford OX1 3AN, UK

[2]School of Geography, Earth and Environmental Sciences, University of Birmingham, Edgbaston, B15 2TT, England.

[3]Department of Earth Sciences, The Natural History Museum, London, SW7 5BD, UK

[4]Department of Natural Sciences, National Museum of Scotland, Old Town, Edinburgh, Chambers Street, Edinburgh, EH1 1JF, Scotland.

[5]School of Earth Sciences, University of Bristol, Wills Memorial Building, Queen's Road, Bristol, BS8 1RJ, England.

[6]Institute of Biodiversity, Animal Health and Comparative Medicine, College of Medical, Veterinary and Life Sciences, University of Glasgow, University Avenue, Glasgow, G12 8QQ, Scotland.

[7]Bayerische Staatssammlung für Paläontologie und Geologie, Munich, Germany

[8]Museum of Paleontology and Department of Earth and Environmental Sciences, University of Michigan, Ann Arbor, MI 48109-1079, USA.

Short title: Cranial anatomy of *Martillichthys*

ABSTRACT

Our understanding of the ecology and phylogenetic relationships of Pachycormiformes, a group of Mesozoic stem teleosts including the iconic *Leedsichthys*, has often been hindered by a lack of comprehensive morphological information. Micro-CT scanning of an articulated, though flattened, cranium of the edentulous *Martillichthys renwickae* from the Middle Jurassic (Callovian) Oxford Clay of the UK reveals previously unknown internal details of the most complete suspension-feeding pachycormiform skull known, including the palate, braincase, and branchial skeleton. The latter preserves gill rakers with elongate, pointed projections similar to those of *Asthenocormus*, in contrast to the finer fimbriations associated with *Leedsichthys*. We also reinterpret some previously described features, including dermal bone patterns of the snout, skull roof, and lower jaw, and the morphology of the ventral hyoid arch. These new anatomical data reinforce the phylogenetic placement of *Martillichthys* as part of the Jurassic clade of edentulous pachycormiforms. The elongated skull geometry of these Jurassic taxa is strikingly similar to that of *Ohmdenia*, the sister taxon to edentulous pachycormiforms, but contrasts sharply with the morphology of the Late Cretaceous edentulous pachycormiform *Bonnerichthys*, raising questions over the phylogenetic relationships among these taxa. Most significantly, *Martillichthys* shows specialized characters with a restricted phylogenetic distribution among suspension-feeding pachycormiforms, including the distinctive gill rakers and a greatly extended occipital stalk. Our analysis of *Martillichthys* supports past interpretations of a close relationship with *Asthenocormus*, and provides a model for interpreting the less complete remains of other members of this enigmatic group of fishes.

Key words. Martillichthys, Pachycormiformes, CT-scanning, fossils, ecology, evolution

INTRODUCTION

Pachycormiformes is a clade of neopterygian fishes that ranges in age from the Early Jurassic (Toarcian; Lehman 1949) to the end of the Late Cretaceous (Maastrichtian; Friedman 2012*b*; Friedman *et al.* 2013), and represents an early-diverging lineage of stem teleosts (Patterson 1973, 1994; Arratia 2004; Friedman *et al*. 2010; Friedman 2012*a*). Pachycormiform morphology is distinctive, with members of the group united by a number of synapomorphies: a compound bone (rostrodermethmoid) forming the anterodorsal border of the mouth; a reduced coronoid process of the mandible; absence of supraorbitals associated with a dermosphenotic defining the dorsal margin of the orbit; two large, plate-like suborbital bones posterior to the infraorbitals; long, slender pectoral fins (see Liston & Maltese 2016 for a critique of past descriptions of 'scythe-like'); asymmetrical branching of pectoral-fin lepidotrichia; considerable overlap of the hypurals by caudal-fin rays (hypurostegy); and the presence of distinctive uroneural-like ossifications of the caudal-fin endoskeleton (Mainwaring 1978; Lambers 1988, 1992; Arratia & Lambers 1996; Kear 2007; Friedman *et al*. 2010; Friedman 2012*a*; Arratia & Schultze 2013). Pachycormiforms are widely distributed, with abundant material known from Europe and North America (Stewart 1988; Friedman *et al.* 2010; Wretman *et al.* 2016) and rarer remains from South America, Australia, the Middle East, and most recently Antarctica (Woodward 1895; Kear 2007; Gouiric-Cavalli 2013; Gouiric-Cavalli & Cione 2015; Wretman *et al*. 2016; Gouiric-Cavalli 2017; Cione *et al.* 2018; Gouiric-Cavalli *et al.* in press). Material from Myanmar previously identified as pachycormiform has recently been reinterpreted as atselfatiiform (Taverne & Liston 2017). Many pachycormiform fossils are known from well-preserved, articulated or associated specimens, with numerous examples from famous *Lagerstätten* including the Early Jurassic (Toarcian) Posidonia Shale of Germany (Hauff 1953) and Strawberry Bank of the UK (Williams *et al*. 2015; Cawley *et al.* 2018), the Middle Jurassic (Callovian) Oxford Clay of the UK (Martill 1986), the Late Jurassic plattenkalks of Germany and France (Barthel *et al*. 1990; Lambers 1992), and the Late Cretaceous (Coniacian-Campanian) Smoky Hill Chalk of the USA (Stewart 1988, 1990). Despite this abundance of material, most pachycormiforms remain poorly known, with the clade represented by only a single operational taxonomic unit (generally *Pachycormus*

macropterus) in many analyses of neopterygian or teleost relationships (e.g. Arratia 2004; López-Arbarello & Sferco 2018).

The lack of comprehensive morphological information is particularly acute for edentulous pachycormiforms, a presumed clade of large-bodied (> 2 m in total length) taxa interpreted as Mesozoic analogues of mysticete whales and suspension-feeding chondrichthyans (Friedman *et al*. 2010). Its members range in age from the Middle Jurassic to the Late Cretaceous, and currently include five recognized genera: the Jurassic *Asthenocormus* (Quenstedt 1852), *Leedsichthys* (Woodward 1889*a*, *b*, 1895), and *Martillichthys* (Liston 2006, 2008*a*); and the Cretaceous *Bonnerichthys* (Friedman *et al*. 2010, 2013) and *Rhinconichthys* (Friedman *et al*. 2010). Generically indeterminate material has also been associated with this edentulous radiation (Friedman *et al.* 2010; Cione *et al.* 2018), and a variety of unpublished remains are also known. Considerable interest centers on the paleobiology of these giant pachycormiforms and their role in ancient marine ecosystems (Martill 1988; Liston 2006; Friedman *et al*. 2010; Friedman 2012*a*; Liston *et al*. 2013; Ferrón *et al.* 2018; Gouiric-Cavalli *et al.* in press). Unfortunately, large size, combined with reduced ossification relative to other pachycormiforms (taken to an extreme in *Leedsichthys* and *Bonnerichthys*), makes them difficult subjects for detailed anatomical study, with even the best-known taxa only described in limited detail. *Rhinconichthys* is known from three incomplete skulls (Friedman *et al*. 2010; Schumacher *et al*. 2016), while *Bonnerichthys* and *Leedsichthys* are represented principally by isolated remains with rare associated but disarticulated individuals (Friedman *et al*. 2010; Liston 2016). In contrast to the incomplete nature of most edentulous pachycormiform fossils, there is a nearly complete specimen of *Martillichthys* (Liston 2008*a*) and several articulated individuals of *Asthenocormus* (Lambers 1992). These taxa therefore serve an important role in interpreting the more incomplete remains of their close relatives, which is vital to better constraining the evolutionary history and paleobiology of this enigmatic but ecologically significant radiation.

Here we use micro-CT (μCT) scanning to redescribe the cranial anatomy of the holotype of *Martillichthys renwickae* (Fig. 1). Our study emphasizes concealed aspects of internal structure not accessible by previous, external examinations (Liston 2008*a*), with the principal goals of improving our understanding of *Martillichthys* itself and using this new description to make inferences about the ecology and evolution of both *Martillichthys* and the broader clade of edentulous pachycormiforms. It is our hope that a more detailed account of *Martillichthys* will serve as an anatomical 'Rosetta Stone' for interpreting structure in less complete or more fragmentary remains of its relatives.

MATERIALS AND METHODS

Materials

Pachycormiformes

Bonnerichthys gladius. KUVP 60692, University of Kansas Natural History Museum. Disarticulated skull, pectoral girdles, and fins from the Coniacian-Santonian Smoky Hill Chalk Member of the Niobrara Formation of Kansas, USA. This specimen was studied on the basis of uncatalogued casts kept in the University of Michigan Museum of Paleontology.

Leedsichthys problematicus. NHMUK P.6921, Natural History Museum, London, UK. The holotype specimen, comprising disarticulated remains of the skull, pectoral girdle, and postcranium. This specimen is from the Callovian Oxford Clay of Peterborough, UK.

Leedsichthys problematicus. NHMUK PV P.10156, Natural History Museum, London, UK. An articulated set of ventral branchial arches plus the left hyomandibula. This specimen is from the Callovian Oxford Clay of Peterborough, UK.

Martillichthys renwickae. NHMUK PV P.61563P, Natural History Museum, London, UK. The holotype specimen comprising a nearly complete articulated individual. An additional specimen attributed to *Martillichthys* is housed in the Peterborough Museum (PETMG F161), but this individual is encased in a dense concretion that is likely not amenable to μCT using most laboratory-based machines (pers. obs. MF of similarly preserved fishes from the Oxford Clay Formation).

Pachycormus sp. NHMUK PV OR 32433, Natural History Museum, London, UK. Three-dimensionally preserved skull from the Toarcian of Curcy (Normandy, France). This specimen was μCT scanned in January 2016.

Pachycormus sp. BRLSI M1297, Bath Royal Literary and Scientific Institution, Bath, UK. Three-dimensionally preserved cranium and pectoral girdle from the Toarcian deposits of Strawberry Bank Lagerstätte in Ilminster (Somerset, UK). This specimen was μCT scanned in June 2017.

Pachycormus sp. BRLSI M1361a, Bath Royal Literary and Scientific Institution, Bath, UK. Three-dimensionally preserved cranium and pectoral girdle from the Toarcian deposits of Strawberry Bank Lagerstätte in Ilminster (Somerset, UK). This specimen was μCT scanned in July 2015 and again in February 2017.

Protosphyraena sp. FHSM VP-3251, Sternberg Museum of Natural History, Fort Hays State University, Hays, Kansas, USA. Disarticulated specimen comprising incomplete remains of skull and pectoral girdle from the Coniacian-Santonian Smoky Hill Chalk Member of the Niobrara Formation of Kansas, USA.

Methods

NHMUK PV P.61563P was scanned using a Nikon Metrology HMX ST 225 CT scanner at the Natural History Museum, London. The X-ray beam was generated with a current of 150 μa and voltage of 190 kV, and a 1 mm copper filter was used. Resolution of the scan was 126 μm. The length of the specimen exceeded the maximum field of view for the scanner, so the fossil was imaged in two sections using identical machine settings. Image stacks for these separate scans were then spliced to create a single tomogram stack for segmentation.

The resulting dataset was loaded into Mimics Innovation Suite V.18.0 (http://biomedical.materialise.com/mimics; Materialise, Leuven, Belgium), which was used to segment individual skeletal elements. Data objects were imported into Blender V.2.77a (http://www.blender.org; Blender Institute, Amsterdam, Netherlands) for reconstruction, description and imaging. Limitations arise

from damage to or loss of some bones (particularly around the cheek), very close application of adjacent ossifications that obscures their boundaries (particularly the skull roof, braincase and parasphenoid), and difficulties distinguishing bone from matrix in tomograms from some regions of the skull.

Anatomical conventions

In order to facilitate comparison with other descriptions, we use conventional actinopterygian terminology to describe the skull roofing bones (see Gardiner & Schaeffer 1989 and Gardiner *et al.* 2005 for discussion of homology between actinopterygian and sarcopterygian skull bones.).

SYSTEMATIC PALAEONTOLOGY

ACTINOPTERYGII Cope, 1887

NEOPTERYGII Regan, 1923

TELEOSTEI Müller, 1845

PACHYCORMIFORMES Berg, 1937

PACHYCORMIDAE Woodward, 1895

Genus *Martillichthys* Liston, 2008*a*

Martillichthys renwickae Liston, 2008*a*

1984 *Asthenocormus* sp. Schaeffer & Patterson, p. 74–75.

1991 *Asthenocormus* sp. Martill, p. 220–222, plate 44.

2008*a* *Martillichthys renwickae* Liston, p. 184–192, figs. 3, 4.

Institutional abbreviations. BRLSI, Bath Royal Literary and Scientific Institution, Bath; KUVP, University of Kansas Museum of Natural History, Lawrence, Kansas; NHMUK, Natural History Museum, London; PETMG, Peterborough Museum and Art Gallery, Peterborough, Cambridgeshire.

Type specimen. NHMUK PV P.61563, *Martillichthys renwickae.* A nearly complete individual, from Bed 12 of the Oxford Clay Formation at the Dogsthorpe Pit, Peterborough, England (Martill 1986). This corresponds to the Tethyan middle Callovian ammonite zones *Reineckia anceps* to *Erymnoceras coronatum* (Martill 1991, fig 1.2). On this basis, the fossil is assigned an age range of 164.63 Ma to 167.97 Ma (Gradstein *et al.* 2012; table 26.3).

Referred material. PETMG F161, *Martillichthys renwickae*. An unprepared specimen in a concretionary nodule consisting of the cranium and extending to the posterior edge of the base of the pectoral fins.

Diagnosis. The following combination of characters distinguish *Martillichthys* from other edentulous pachycormiforms: canal-bearing rostrodermethmoid; posterior process of rostrodermethmoid extending between frontals; gap between frontals; elongate, pointed gill rakers; body of gill rakers club-like rather than tapering to a pointed, distal tip; hyomandibula with plate-like rather than cylindrical dorsal head; hyomandibula less than one third the length of the mandible; elongate preorbital region; elongate occipital stalk; deep groove for the dorsal aorta in the occipital stalk.

Remarks. Previous analyses have been unable to resolve the relationships between *Martillichthys*, *Leedsichthys* and *Asthenocormus*. Liston (2006, 2008*a*) noted many similarities between these taxa, and subsequent cladistic analyses placed the three in an unresolved polytomy (Friedman *et al*. 2010; Friedman 2012*a*). Distinguishing these genera is complicated by a poor understanding of anatomy in *Leedsichthys* and, to a lesser degree, *Asthenocormus*. The most conspicuous difference between *Asthenocormus* and *Martillichthys* concerns the geometry of the contact between the rostrodermethmoid and the frontals. This is depicted as transverse for *Asthenocormus* (Lambers 1992), but is ‘v’-shaped in *Martillichthys*. At present, the few aspects of overlapping anatomy in the diagnosis of *Martillichthys* and *Leedsichthys* do not show striking differences with the exception of some aspects of the skull roof (see Liston 2008*a*, fig. 6). More

detailed description of *Leedsichthys* will be vital in more clearly differentiating *Martillichthys* from this taxon.

MORPHOLOGICAL DESCRIPTION

In order to facilitate comparison with other descriptions, we use conventional actinopterygian terminology to describe the skull roofing bones (see Gardiner & Schaeffer 1989 and Gardiner *et al.* 2005 for discussion of homology between actinopterygian and sarcopterygian skull bones.). The skull is approximately 484 mm long and measures 142 mm at its widest point. Strong dorsoventral compression has resulted in a maximum specimen depth of only 28 mm (Figs. 1, 2).

Skull roof

Many of the margins between the dermal bones of the skull roof are not discernable in µCT tomograms and divisions are therefore distinguished based on external observation of the fossil. The geometry and position of sutures is approximate, as these show a deeply interdigitating pattern that appears confluent with the fibrous texture of individual bones.

A wedge-shaped bone of uncertain identity is sutured to the right anterolateral margin of the rostrodermethmoid (?Ant, Fig. 2*a*, Fig. 3*a, b*). The dorsal surface is smooth, and a narrow ridge along the anterior margin of the ventral surface (R, Fig. 3*c, d*) closely follows the anterior margin of the tentatively-identified premaxilla. The left posterior corner bears a small notch that aligns with a notch in the rostrodermethmoid (?Nos, Fig. 3*a, b*). These notches appear to be present on both sides of the rostrodermethmoid, and presumably frame the anterior naris. This bone shows no obvious indications of grooves or canals, but it is positionally equivalent to the antorbital.

The large rostrodermethmoid is broken into two pieces (Rde, Figs. 2*a, b,* 4*a, b*); when reconstructed, the complete bone is roughly diamond-shaped, broader anteriorly and gradually tapering to a posterior projection that extends between the frontals (Rde, Figs. 2*a, b,* 4*a, b*). Two shallow grooves extend along the dorsal surface of the rostrodermethmoid (Su.C, Fig. 3*a*), aligned with the long axis of the frontals and converging towards the midline anteriorly but not intersecting. We interpret these as indicating the course of the supraorbital sensory canals, which are ordinarily borne on the nasals. There is no indication of an ethmoid commissure.

The paired frontals are elongate. The mesial margin is straight, and each frontal gradually broadens posteriorly (Fr, Fig. 4*a, b*). The frontals are widest at roughly two-thirds of their length, at which point they are separated by a median gap (Fr.Gp, Fig. 4*a, b*). This gap extends to the posterior margins of the frontals. The frontals show no traces of sensory canals. A small triangular bone whose mesial margin sutures with the lateral margin of the right frontal might represent a fragment of the nasal, but bears no trace of grooves or a buried canal, making a positive identification difficult (?N, Figs. 2, 4; see below in 'Cheek, circumorbital bones and sclerotic ossicles').

The parietals are paired, rectangular bones that suture with one another along the midline, and with the frontals anteriorly. They are roughly one third of the length of the frontals (Par, Fig. 4*a, b*). The posterior margin of the skull roof has a scalloped margin, with projections formed by the posterolateral corners of the dermopterotics and posteromesial margins of the parietals at the midline (Fig. 3*f*). No obvious grooves are present on the dorsal surface of the parietals, which are smooth and unornamented.

Triangular dermopterotics flank the lateral margin of each parietal, and extend anteriorly to contact the posterior third of the lateral margin of each frontal (Dpt, Fig. 4*a, b*). The posterolateral corner of each dermopterotic is produced as a small posterior process that forms the lateral prong of the scalloped posterior edge of the skull roof (Fig. 4*a, b*).

Braincase, parasphenoid, and associated bones

The braincase is strongly dorsoventrally compressed and cannot be easily distinguished from the overlying skull roof in tomograms. It is similarly difficult to separate the braincase and parasphenoid, although the boundaries between the two are easier to identify in the orbital and ethmoid regions. Sutures between individual ossifications of the braincase are not visible, so only the general morphology of major regions of the braincase can be described. The ethmoid and sphenoid regions of the braincase are largely concealed by the skull roof dorsally, and the broad, spatulate anterior corpus of the parasphenoid ventrally (Fig. 4). Flattening of the skull is so severe that anatomy of the braincase can only be described in ventral view.

The anteroposteriorly extensive lateral ethmoids are visible as slender bands of bone extending beyond the lateral margins of the frontals and the parasphenoid (L.Eth, Fig. 4). The posterior edge of the lateral ethmoid defines the anterior margin of the orbit (Fig. 2*a, b*). There is no clear indication of the median ethmoid ossification, or any of its associated structures (e.g. nasal pits).

The postorbital processes mark the rear margin of the orbit. Their relative position indicates a long preorbital region of the skull, with posteriorly-placed eyes (P.Op.Pr, Fig. 4*c, d*). The ventral surface of the otic region shows little detail. This portion of the braincase extends to the lateral edge of the dermopterotics, but has been flattened *post-mortem*. A strap-shaped facet for the articulation of the hyomandibula is visible near the lateral edge of the neurocranium on both sides of the skull (H.Fa, Fig. 4*c, d*). The occipital region is the only region of the neurocranium visible in both dorsal and ventral view. It is dominated by a long basioccipital 'stalk' (Boc, Fig. 4*a*), which protrudes from the posterior edge of the braincase and extends well beyond the rear margin of the skull roof. The stalk is truncated by breakage at the end of the specimen, and so would have been more extensive. A shallow groove for the dorsal aorta extends along the ventral midline of the stalk (A.G, Fig. 4*c, d*), while its open, gutter-like dorsal surface presumably accommodated the notochord

(Nc.G, Fig. 4*a, b*). Exoccipitals are visible dorsally, lying immediately posterior to the rear margin of the skull roof (Eco, Fig. 4*a*, *b*) and flanking the foramen magnum (?Fm, Fig. 4*a, b*).

The parasphenoid is long and distinctive in shape. The broad, spatulate anterior corpus of the bone extends at least half of the overall length of the skull, but its anterior margins are not clear. The widest point of the anterior corpus is located at approximately mid-length, where it is equal in width to the frontals, but it is difficult discern the anterior margin of much of the parasphenoid due to the crushed nature of the specimen (Psp, Fig. 4*c*, *d*). The corpus becomes medially constricted in the orbital region of the skull. The ventral surface of the anterior corpus bears no obvious teeth or denticles, but is concave, forming an arched roof to the buccal cavity. The posterior stalk of the parasphenoid underlies the otic and occipital regions of the braincase, although its margins are difficult to discern in μCT data. It appears that the parasphenoid only extends part of the length of the basioccipital stalk, terminating slightly posterior to the dermopterotic processes (Fig. 4*c, d*). The ascending process and basipterygoid process of the parasphenoid cannot be identified, nor can the presence or absence of foramina in the bone associated with basicranial circulation be established.

A thin, plate-like ossification lies anterior to the parasphenoid and ventral to the rostodermethmoid. Although posteriorly distinguishable from the overlying braincase and skull roof (Fig. 4*e*), it is impossible to identify a boundary between these ossifications anterior to a point just behind the narial opening. A slight thickening at the anteriormost tip of the flattened skull roof and braincase (T.P., Fig. 3*c*, *d*) might be associated with this bone, and the shape of its posterior margin suggests that it may interdigitate with the parasphenoid. Based on its position ventral to the braincase and anterior to and at roughly the same level as the parasphenoid, we tentatively identify it as a median vomer (M.Vmr, Fig. 4*c*, *d*).

Upper jaw

The upper jaw is represented by the maxilla and premaxilla, and there is no indication of a supramaxilla. The maxilla is half the length of the mandible, and roughly three times as long as deep (Mx, Fig. 5). The maxilla is rod-like anteriorly, with a circular cross section, but flattens into a concave plate posteriorly, which is applied to the dorsolateral surface of the mandible (Fig. 5*a*). In lateral view, the maxilla bears a small prong at its posterodorsal corner (P.P, Fig. 5*b*-*g*), and the anterior tip bears a small articular process (A.Pr, Fig. 5*b*-*g*). The anterodorsal margin has a slightly thickened ridge, which sits slightly above the rest of the dorsal margin of the bone (T.R, Fig. 5*b*-*g*). Due to disarticulation during preservation, it is unclear how the maxilla would have articulated with the rest of the skull (Fig. 2*a*, *b*).

A splint-like bone, preserved underneath other dermal bones of the snout on the right side of the fossil, is interpreted as a premaxilla (?Pmx, Fig. 3*c*, *d*). The posterior and medial margins of the bone are incomplete. The preserved fragment is roughly two-thirds of the length of the antorbital, but its true length and width is difficult to discern.

Mandible

Five major bones contribute to the mandible: dentary, angular, surangular, prearticular and articular (Fig. 6). These are joined by what is apparently a single coronoid, although sutures between bones are difficult to resolve in tomograms (Fig. 6*a*-*c*).

The dentary is the principal bone on the outer face of the mandible (Dent, Fig. 6*d, e*). Each dentary is gently bowed anteriorly, meeting at a rounded symphysis, and a thumb-shaped depression lies near the anterior margin of each. The dentary contributes only a narrow band to the dorsal surface of the mandible, and this oral margin bears no teeth or denticles. The cross-sectional profile of the dentary is ‘r’-shaped, with a mesial ridge abutting the lateral margin of the coronoid (Fig. 6*b, c*).

Posteriorly, the dentary sutures with the surangular and angular (Sang, Ang, Fig. 6*d*-*g*). In lateral view, the angular is long and wedge-shaped, roughly half the length of the dentary, and tapers to an point halfway along the mandible. The lateral surface of the angular bears two grooves, marking the path of the mandibular sensory canal, which extend parallel to the ventral margin of the jaw and continue on the dentary (MSC, Fig. 6*d, e*). The surangular forms the posterodorsal corner of the external surface of the jaw, and sutures with the dentary anteriorly and the angular ventrally. Midway along the adductor fossa, the dorsal margin of the mandible bears a reduced coronoid process (Cor.Pr, Fig. 6*f*, *g*) composed solely of the surangular.

The wedge-shaped prearticular covers most of the mesial surface of the mandible (Part, Fig. 6*f, g*). It defines the anterior margin of the adductor fossa (Ad.F, Fig. 6*f*, *g*), meeting the surangular posterior to the coronoid process, and attaches to the articular posteriorly. The exposed surface of the prearticular is smooth, and free of denticles.

The coronoid series of *Martillichthys* appears to be represented by a single bone, with no clear sutures (Cor, Fig. 6*b*, *c*, *f, g*). The coronoid can be divided into two principal regions. The more anterior is a bulbous expansion that forms a deeply interdigitated, subvertical suture with the prearticular and a horizontal suture with the inner face of the dentary. The more posterior consists of a long, rod-shaped portion that lies dorsal to the dentary and prearticular, extending from approximately mid-length of the mandible to near the symphysis.

The articular lies at the posterior end of the jaw (Art, Fig. 6*d*–*g*). It is flanked laterally by the surangular and angular, and mesially by the prearticular. The articular defines the posterior margin of the adductor fossa, and bears a well-defined glenoid fossa for the articular condyle of the quadrate (Gl.F, Fig. 6*d*-*g*). The jaw joint is only slightly above the ventral margin of the mandible, and is oriented posteriorly.

Gill skeleton

The basibranchials, hypobranchials, and ceratobranchials are preserved (Fig. 7*a, b*). Only a single, elongate basibranchial (?BbIII-IV; Fig. 7*a*) appears present, but its complex shape and position between multiple hypobranchials suggests that it may represent the fusion of multiple basibranchials.

Mineralized hypobranchials are only apparent for the first two branchial arches (HbI-II, Fig. 7*a, b*). Hypobranchial I is largely straight but curves gently towards its antimere, anterior to the basibranchial. The anterior region is expanded into an articular facet, and a longitudinal groove is visible posterior to this anterior expansion. Hypobranchial II is of a similar length and width to hypobranchial I, although the anterior end is less expanded and the ventral groove less defined.

Five ceratobranchials are present. A gap midway along their length represents a break in the specimen, and the posterior ends are truncated by the end of the block containing the skull (CbI-V, Fig. 7*a, b*). Ceratobranchials I and II articulate with hypobranchials I and II respectively. There are substantial gaps between the anterior ends of the remaining ceratobranchials and the basibranchials, indicating that intervening hypobranchials were likely present but unmineralized. The first four ceratobranchials are morphologically similar. Each is a long, thin bone, about three times the length of the basibranchial. The ceratobranchials are 'n'-shaped in cross-section, with a longitudinal groove extending along the ventral side. The fifth ceratobranchials are the shortest of all the series, approximately half the preserved length of the fourth pair and a third of the length of the first (Fig. 7*a, b*).

In contrast to the ventral gill skeleton, which is truncated posteriorly, the dorsal gill skeleton appears to be largely complete within the block containing the skull (EbI-IV, Figs. 2*a, b*, 7*c, d*). Four pairs of epibranchials are present on the right side of the specimen, but only three are preserved on the left (Fig. 7*c, d*). However, only the posterior portion can be observed, and as such the presence or absence of uncinate processes cannot be determined. The epibranchials are shorter than the ceratobranchials, and each is shorter than the element

anterior to it. Apart from this difference in size, each ceratobranchial shows a broadly similar morphology: slender with a pronounced dorsal groove giving the bone a ‘u’-shaped cross-section.

Tooth plates have not been observed in association with the gill skeleton, but numerous elaborate gill rakers are present (G.R, Fig. 7*a, b, e–n*). Each raker comprises a long, club-shaped stalk (Liston 2013) that articulates with the gill skeleton, and bears elongate, pointed projections. The length of each projection is understated in CT renders due to limitations associated with a large (126 µm) voxel size, but the true length—up to 0.5 cm —is apparent from external consideration of the fossil (Fig. 7*a, b, e–n*). The rakers are directed anterolaterally, and are oblique to the rest of the gill skeleton (Fig. 7*a, b*). They are relatively large, roughly a fifth of the length of the hypobranchials, and extremely numerous: at least 110 are present. The projections extend from the anterior margin of each raker along roughly a quarter of the length (Fig. 7*e–m*). Based on the regular spacing between some of the rakers, and their alignment with the ventral ceratobranchials, we estimate that there are approximately 15 rakers per ventral gill arch.

Hyoid arch and palate

The hyoid arch of *Martillichthys* comprises hypohyals, anterior and posterior ceratohyals, interhyals, and hyomandibulae. The hypohyals are laterally flattened, with a rounded profile, and lie close to the midline of the fossil (Hhy, Fig. 8*a, b*). Each hypohyal curves gently towards its antimere. Approximately halfway along the ventral edge, a small foramen marks the course of the afferent hyoid artery (AH.A.F, Fig. 8*a, b*).

The hypohyals articulate with the elongate anterior ceratohyals posteriorly (A.Chy, Fig. 8*a, b*). These are roughly four times the length of the hypohyal and nearly half the length of the entire skull (Fig.2*c, d*). They are straight and laterally compressed, with a medial constriction. A longitudinal groove extending along the posterior half of the lateral face of each ceratohyal indicates the path of the afferent hyoid artery (AH.A.G, Fig. 8*a*, *b*).

The posterior ceratohyals articulate with the anterior ceratohyals (P.Chy, Fig. 8*a, b*), and are wedge-shaped, matching the depth of the anterior ceratohyals anteriorly but tapering posteriorly. The longitudinal grooves of the anterior ceratohyals continue on to the posterior ceratohyals.

The trapezoidal interhyals are the smallest bones of the hyoid arch, and lie between the posterior ceratohyal and the ventral portion of the hyomandibula (Ihy, Fig. 8*a, b*). The interhyal on the right side appears to be more completely preserved (Fig. 2*c, d*).

The following bones of the suspensorium are preserved on the left side of the specimen: the entopterygoid, metapterygoid, ectopterygoid, quadrate and symplectic (Fig. 8*c, d*). Only the quadrate, symplectic, and hyomandibula are present on the right side of the skull.

The quadrate (Quad, Fig. 8*c*, *d*) is dominated by its well-developed articular head (MQ.J, Fig. 8*c, d*). The posteroventral margin of the bone bears a sharp notch approximately a third of the way along its length, into which the rod-like symplectic inserts. The symplectic is approximately the same length as the quadrate but half as wide until the posterior third, which is twice as wide as the rest. Both the right and left symplectic are broken approximately two-thirds of the way along their length (Sym, Fig. 8*c, d*).

The toothless ectopterygoid is boomerang-shaped (Ectp, Fig. 8*c, d*). The broad posteroventral limb forms a tight sutural connection with the anterodorsal margin of the quadrate. The anterodorsal limb is more slender, and terminates in a pointed tip. The metapterygoid has broken into three pieces: one applied to the quadrate and ectopterygoid; one lateral to the entopterygoid and separated from the more anterior bone by a small crack (Mpt, Fig. 8*c*, *d*); and one separated by a further small gap and applied to the anterior margin of the hyomandibula (Fig. 2*c, d*). The oval entopterygoid contacts the ectopterygoid ventrally and the metapterygoid posteriorly (Entp, Fig. 8*c, d*). The inner surface of the entopterygoid is smooth, with no evidence of denticles.

The hyomandibula is plate-like, roughly rectangular in shape and lies on a slightly diagonal axis relative to the remainder of the skull (Hyo, Figs. 2*c, d*, 8*a, b*, e–*h*). It is medially constricted, with a waisted appearance in lateral view (Fig. 8*e–h*), and the distal end is expanded to a much greater degree than the proximal head. Although not preserved, a thickened ridge of bone in the posterodorsal portion of the hyomandibula, identified through external analysis, suggests that an opercular process was originally present. A foramen in the upper third of the bone marks the passage of the hyomandibular branch of the facial nerve (FN.F, Fig. 8*a*, *b*).

Cheek, circumorbital bones and sclerotic ossicles

Preserved components of the cheek include the infraorbitals, suborbitals, dermosphenotic and preoperculum, as well as fragments of dermal bone that are harder to identify. On the left side of the fossil, midway along the orbit, a square fragment of bone articulates with the lateral margin of the frontal. Comparison to other pachycormids indicates that a dermosphenotic identity is most likely, although the lack of a sensory canal means that a supraorbital identity cannot be discounted (?Dsp, Fig. 2). Multiple bones surrounding the orbit are preserved on the right side of the skull, but are displaced from life position (Fig. 9). The dermosphenotic is broken into two pieces, but indicates that the complete bone would have framed the posterodorsal and dorsal margins of the orbit (Dsp, Fig. 9*a*, *c-d*). As preserved, the bone appears triradiate, with a long anterior arm and short posterior and ventral arms; the dorsal margin of the anterior arm closely matches the lateral margin of the skull roof in the orbital region. A portion of the sensory canal is visible on the posterior fragment of the dermosphenotic (S.C., Fig. 9*c-d*). At least two plate-like bones lie posterior to the orbit, with four more slender ossifications spread across the orbital region. The larger, more posterior bones are interpreted as possible suborbitals (?Sor, Fig. *9b*). Two curved bones in the middle of the orbital region represent an incomplete sclerotic ring. The larger ossicle is approximately one-eighth of the overall skull length (D.Sco, Fig. 9). The smaller ossicle appears to be broken (V.Sco, Fig. 9). The remaining splint-like bones in the orbital region are likely infraorbitals (?Ior, Fig. 9*a, c-d*).

A small fragment of the preoperculum is preserved on both sides of the skull (Pop, Fig. 8*c, d*). It is thin, closely applied to the lateral surface of the quadrate, and bears a fimbriate posterior margin. No canals or grooves for the preopercular sensory canal are visible.

Operculogular series

The operculogular series consists of the gular plate, branchiostegal rays, operculum and suboperculum. From external analysis, at least 27 branchiostegal rays are present between the hypohyal and anterior ceratohyal, with the series extending along the posterior ceratohyal (Bs.R, Figs. 1*a*, 8*a*, *b*). A total count is not possible, and due to their thinness the branchiostegals are not visible in tomograms or associated renders.

The gular plate lies immediately posterior to the mandibular symphysis and ventral to the rostrodermethmoid (Gul, Fig. 2*c*, *d*). The plate is exceedingly thin near its posterior margin, and terminates with a ragged edge. It is possible that the bone extended further posteriorly, but this weakly mineralised portion was either not preserved or lost during specimen preparation. This posterior region is too think to be visualized in tomograms, and while visible externally (Fig. 1*a*) it is not apparent in renders (Fig. 2*c*, *d*) As preserved, it extends approximately half the length of the intermandibular space, covering the hypohyals (Fig. 1*a*). By contrast, the thicker region of this bone that is apparent in tomograms is restricted anterior to the hypohyals (Fig. 2*c*, *d*). A series of ridges and grooves cover the gular plate, radiating from a smooth region at the center of the ventral surface of the bone (Fig. 2*c, d*).

The plate-like operculum and suboperculum are preserved on the left side of the fossil, but their margins are incomplete, in addition to being posteriorly truncated (Fig. 2*c, d*). The operculum (Op, Fig. 2*c, d*) slightly overlaps the dorsal edge of the suboperculum. The suboperculum terminates posterior to the rounded posterior margin of the hyomandibula (Sop, Fig. 2*c, d*). Due to incomplete preservation, little can be said about the relative sizes of these bones.

DISCUSSION

Revisions and additions to previous descriptions

Our study of *Martillichthys* provides new information on previously concealed internal anatomy, as well as clarifying some aspects of features only partially exposed at the surface of the specimen. This permits an update of some anatomical interpretations of *Martillichthys* given in earlier accounts (Martill 1991; Liston 2008*a*).

Skull roof. Reexamination of the specimen permits clarification of several features of the skull roof. We identify a gap between the frontals in *Martillichthys*. A similar opening has been identified between the frontals of the Late Cretaceous pachycormiform *Rhinconichthys taylori* (Schumacher *et al.* 2016), and as either extending between the parietals, or being restricted between the parietals, in *R. uyenoi* and *R. purgatoirensis* respectively (Schumacher *et al.* 2016, fig. 8). Geometry of the frontals suggest that a similar gap might also have been present in *Bonnerichthys* (Friedman *et al.* 2010), although separation between skull roofing bones in this taxon raises questions about equivalence of the condition. Such a gap has not been reported in *Asthenocormus* (Lambers 1992), and is absent in tooth-bearing pachycormiforms. We also find that the rostrodermethmoid of *Martillichthys* is diamond-shaped rather than triangular, and that the dermopterotic extends anterior to the transverse suture between the frontals and parietals rather than terminating at the level of this junction (Liston 2008*a*). This is in broad agreement with conditions in most other pachycormiforms and outgroups.

Our interpretation of the identity, geometry, and arrangement of bones contributing to the snout also differs from previous accounts. Liston (2008*a*) interpreted the rostrodermethmoid of *Martillichthys* as a narrow, triangular bone, contacting the frontals via a transverse suture and excluded from the gape by long, slender nasals that contacted one another at the midline. Based on our scan data, we reinterpret the sutures between the rostrodermethmoid and nasals as grooves for the supraorbital sensory canals, borne entirely on the body

of the rostrodermethmoid. This brings the overall geometry of the rostrodermethmoid more into line with that seen in other pachycormiforms, where this bone contacts the upper jaw. Presence of the supraorbital sensory canal on the rostrodermethmoid suggests either migration of this canal from the nasal to the rostrodermethmoid, or fusion of the nasal and its associated canal with the rostrodermethmoid (see below). Among pachycormiforms, a rostrodermethmoid bearing the supraorbital canal is also found in *Bonnerichthys* (Friedman *et al.* 2010), although in that taxon the canal is buried in the bone in a thickened ridge rather than lying superficially. We also find that the rostrodermethmoid bears a long posterior process that extends between the two frontals, rather than meeting those bones along a gently scalloped margin.

The presence of the presumed supraorbital canal on the rostrodermethmoid complicates the interpretation of more lateral bones of the snout. However, based on conditions in other stem teleosts (e.g. *Dorsetichthys bechei*: Rayner 1948; *Pachycormus macropterus*: Lehman 1949; Mainwaring 1978), we agree with Liston (2008*a*) that the ovoid bone on the right side of the snout is a probable antorbital. Much of Liston's (2008*a*) proposed nasals are, according to our revised interpretation, parts of the rostrodermethmoid. We are only able to identify fragments of dermal bone along the margin of the right frontal as a possible nasal..

Paired vomers are known in the tooth-bearing pachycormiforms *Pachycormus* (Lehman 1949, fig. 4; Mainwaring 1978, fig. 7), '*Hypsocormus*' ('*H.*' *tenuirostris*; Martill 1991, fig. 9.6b), *Orthocormus* (reported as *Hypsocormus* in Rayner 1948, fig. 16), and *Protosphyraena* (Felix 1890, pl. 14; Loomis 1900, pl. 14; Hay 1903, fig. 1). In these taxa, the vomers are splint-like, with their long axes oriented anteroposteriorly. The vomers contact along at least part of their length, and are tightly sutured to one another mesially and, in some taxa, to the parasphenoid dorsally. In some cases, the vomers are so intimately bound to one another and the parasphenoid that their margins are difficult to discern. Vomers have not been previously been identified in *Martillichthys* or any other edentulous pachycormiform. While the structure we interpret as a vomer in *Martillichthys* is median, it is possible that it is composed of paired bones that are too tightly joined to be distinguished in our relatively low-resolution scan. The vomer(s) of *Martillichthys* do not appear to have a

thickened transverse ridge at the anterior margin of the bone, a feature that is ubiquitous among tooth-bearing pachycormiforms.

Upper jaw. The premaxilla was previously unknown in *Martillichthys*. However, we interpret the incompletely-preserved ossification buried beneath the antorbital and contributing to the oral margin of the upper jaw as representing this bone. The position of the putative premaxilla might also be consistent with a vomer (but see above), but the shape of the bone and its overall proportions broadly match the ventrolateral extension of the rostrodermethmoid of *Bonnerichthys*, interpreted by Friedman *et al.* (2010: p.991, fig. 2; pers. obs. of cast of KUVP 60692) as a fused premaxilla. The structure of premaxillae in edentulous pachycormiforms remains poorly known.

As in other pachycormiforms, the maxilla of *Martillichthys* bears an embayment at its posterodorsal corner. This notch marks the position of the supramaxilla in taxa where the bone is present. We have found no trace of a supramaxilla in *Martillichthys*, but this notch is a persistent feature despite the possible loss of the bone that it accommodates in other pachycormiforms. Apart from the absence of teeth, the most striking difference between the maxilla of *Martillichthys* and most other pachycormiforms is the overall geometry of the bone. The maxilla of *Protosphyraena* (FHSM VP-3251) and *Pachycormus* (NHMUK PV 32433) is more slender than that of *Martillichthys*, and the anterior articular process more spur-like.

Mandible. Previous accounts of external anatomy of the lower jaw are largely accurate, although we disagree with past interpretations of the mandible as being structurally very different from that of other pachycormiforms (Liston 2008: p. 186). The major exception is the groove reported by Liston (2008*a*) as a suture between the external dermal bones of the mandible and the prearticular, which instead marks the course of the mandibular sensory canal. The prearticular is confined entirely to the mesial surface of the mandible and is not visible in lateral view. µCT data provides the first clear picture of this bone, along with the coronoid and adductor fossa.

Gill skeleton. The most substantial update to the morphology of the branchial arches relates to the anatomy of the gill rakers and their associated projections. Liston (2008*a*, 2013) reported the presence of rakers and fine raker fimbriations in *Martillichthys*, but concluded that tooth-like extensions from the rakers were absent. However, tomograms reveals that elongate, pointed raker projections similar to those reported in *Asthenocormus* (Lambers 1992: 212; questioned by Liston 2013: 137) are present in *Martillichthys*, rather than the finer fimbriations or oblique edges associated with *Leedsichthys* (Liston 2013; Liston 2008*b*; Gouiric-Cavalli 2017, fig. 2). The presence of these tooth-like projections is also apparent from external observation, refuting past claims that such structures belonged to scavengers rather than *Martillichthys* itself (Liston 2008: p. 191). It is also clear that there is variation between taxa in the geometry of the stalk of the raker (Fig. 10), which is club-like in *Martillichthys* but appears to taper to a point distally in most material attributed to *Leedsichthys* (Liston 2006, figs. 6.1–6.7; Liston 2013, fig 1; Gouiric-Cavalli 2017, fig. 2). While it is possible to determine that the rakers reported in *Asthenocormus* (Lambers 1992, 212, pl. 2*b*) are more morphologically similar to those reported in *Martillichthys* than *Leedsichthys*, they are not complete enough for a more direct comparison.

μCT data also adds detail to the gill skeleton, including the presence of a large basibranchial possibly representing the fusion of III and IV (cf. *Pachycormus* as described by Mainwaring 1978, fig. 13). The absence of basibranchial II indicates that it was cartilaginous, as inferred for other pachycormiforms (e.g. Mainwaring 1978). In addition, we find that the fourth epibranchials identified by Liston (2008*a*, fig. 3) instead represent the dorsal margins of the occipital stalk of the braincase.

Hyoid arch and palate. Our interpretation of the ventral hyoid arch substantially revises that of Liston (2008*a*), which reported minute hypohyals, short anterior ceratohyals, and exceptionally long posterior ceratohyals, roughly the length of the mandible. Instead, we find that the geometry of the ventral hyoid arch in *Martillichthys* more closely agrees with generalized neopterygian conditions in having short hypohyals

and posterior ceratohyals in combination with long anterior ceratohyals (Olsen 1984; Grande and Bemis 1998; Grande 2010). In addition to these updated bone identifications, our scans reveal the presence of an interhyal that is not apparent from external examination.

Cheek, circumorbital bones and sclerotic ossicles. The identity of the disarticulated bones within the orbit requires some discussion. Previous descriptions of *Pachycormus* have identified "at least 10" (Mainwaring 1978: 16) and "at least 11" (Lehman 1949: 10) long, rectangular bones posterior to the orbit as infraorbitals. This arrangement of numerous narrow infraorbitals is generally taken as common to all pachycormiforms, but can only be shown convincingly in a few taxa (e.g. *Euthynotus*: Wenz 1967, fig. 67; *Hypsocormus insignis*: Woodward 1895, fig. 40; '*Hypsocormus*' *macrodon*: Lambers 1992, fig. 17; possibly *Protosphyraena*: Felix 1890, pl. 12). By contrast, larger, plate-like bones posterior to the infraorbitals represent suborbitals (Lehman 1949, fig. 2; Mainwaring 1978, fig. 2). Therefore, we interpret the slender, more anteriorly placed orbital bones of *Martillichthys* as infraorbitals (?Ior, Fig. 9) and the plate-like bones as suborbitals (?Sor, Fig. 9). However, the disruption of their position and the lack of any canals makes these identifications speculative. By contrast, the presence of a sensory canal, combined with the geometry of the bone, clearly establishes the identity of the dermosphenotic. Neither infraorbitals nor suborbitals were identified by Liston (2008*a*), while part of a possible infraorbital was interpreted as a supraorbital (Liston 2008*a*, fig. 3).

Operculogular series. Previously described as having small paired gulars, *Martillichthys* conforms to the general pachycormiform condition in bearing a single large, median gular. The gular commences immediately posterior to the jaw symphysis, encompassing a bone fragment previously interpreted as belonging to the parasphenoid (Liston 2008*a*, fig. 4), and extends posteriorly as a thin, fragmented sheet that covers the anterior half of intramandibular space.

Phylogenetic placement of Martillichthys

Characters resolving Martillichthys *as a pachycormiform.* The monophyly of Pachycormiformes is well-supported by numerous studies that show broad agreement concerning the features uniting the clade (Patterson 1975; Mainwaring 1978; Lambers 1992; Arratia 2004; Liston 2008*a*; Friedman *et al.* 2010; Friedman 2012*a*; Arratia & Schultze 2013; Wretman *et al*. 2016). From this study, we can confirm the following features support the placement of *Martillichthys* as a pachycormiform (Fig. 11; node 1): (1) a compound rostrodermethmoid forming the anterodorsal border of the mouth (*contra* Liston 2008*a*, who interpreted midline contact between the nasals excluding the rostrodermethmoid from the gape); (2) a reduced coronoid process of the mandible; (3) absence of supraorbitals (with the dermosphenotic separating the orbit from the skull roof); and (4) elongate pectoral fins; with (5) distinctive distally bifurcating, asymmetrical, lepidotrichia.

The following features support the placement of *Martillichthys* as an edentulous pachycormiform (Fig 10; node 2): (1) absence of marginal dentition; (2) lack of ornamentation on the dermal bones of the skull; (3) absence of a supramaxilla; (4) broad anterior corpus of the parasphenoid (unlike the narrow corpus reported in *Pachycormus* and most other tooth-bearing pachycormiforms, a broad corpus of the parasphenoid is also seen in *Saurostomus*, which is interpreted as a close relative of edentulous pachycormiforms; Wenz 1967, fig. 65); (5) posterior margin of the parietals form a median projection (unknown in *Bonnerichthys*); (6) absence of a posterior boss on the skull roof (unknown in *Bonnerichthys*); (7) a reduction or loss of scales; and (8) reduction or absence of segmentation in caudal-fin rays (also seen in *Protosphyraena*; McClung 1908; Arratia & Lambers 1995). To this, we add: (9) a gap between the frontals (present in *Rhinconichthys*, equivocal in *Bonnerichthys*, uncertain in *Asthenocormus*; Schumacher *et al.* 2016). A thickened ridge on the lateral surface of the maxilla has previously been cited as a synapomorphy of edentulous pachycormiforms (Friedman *et al.* 2010; Friedman 2012*b*), but this character is highly subjective and we do not regard it as strong evidence for monophyly of the group.

Interrelationships of Martillichthys *and other edentulous pachycormiforms*. Despite limited understanding of most taxa, there are multiple characters that show variable states among edentulous pachycormiforms and might therefore provide clues to their interrelationships. Here we consider the implications of these features, polarizing traits based on conditions observed in proximal (*Pachycormus*: Lehman 1949; Patterson 1975; Mainwaring 1978) and more distal (the early crown neopterygian *Watsonulus*: Olsen 1984) outgroups. We restrict our considerations to edentulous pachycormiforms with the best-known skeletal anatomy: *Asthenocormus* (Lambers 1992), *Bonnerichthys* (Friedman *et al.* 2010), *Martillichthys* (Liston 2008*a*; this study) and *Rhinconichthys* (Friedman *et al.* 2010; Schumacher *et al.* 2016). Less completely known taxa are discussed in the following section.

Our study has both corroborated existing (Friedman *et al.* 2010; Friedman 2012*a*; Wretman *et al.* 2016) and suggested additional synapomorphies uniting edentulous pachycormiforms to the exclusion of *Bonnerichthys* (Fig 10; node 3): (1) elongated occipital stalk (uncertain in *Asthenocormus*); and (2) elongated gill rakers possessing ornamentation such as pointed projections or fimbriations.

Friedman (2012*a*) suggested two characters uniting *Asthenocormus* and *Martillichthys* to the exclusion of other edentulous pachycormiforms. First is the presence of (1) a medially-constricted, or waisted, hyomandibula, which contrasts with the more 'slab-sided' hyomandibulae of *Bonnerichthys* and *Rhinconichthys*. However, the reliability of this character is unclear; a waisted hyomandibula is also present in other pachycormiforms, such as *Pachycormus*, and there is a degree of ambiguity in delimiting the contrasting states of this character. Second, and perhaps more reliably, (2) the posterior process of the dermopterotics is reduced in *Martillichthys* and *Asthenocormus* relative to other pachycormiforms, a condition that contrasts with the extremely long and narrow posterior processes found in *Rhinconichthys* (Fig. 11). To these, we add two characters relating to overall skull geometry highlighted in our study of *Martillichthys*: (3) an elongated pre-orbital region (compared with a proportionally shorter pre-orbital region in *Bonnerichthys*, *Rhinconichthys* and outgroups); and (4) a short hyomandibula relative to the mandible,

comprising less than one third of the lower jaw length (compared with a hyomandibula greater than one third of the length of the mandible in *Bonnerichthys*, *Rhinconichthys* and outgroups).

Set against these characters suggesting a close relationship between *Martillichthys* and *Asthenocormus*, we note other features shared that could suggest alternative hypotheses. First is the proposal by Schumacher *et al.* (2016) that *Martillichthys* and *Rhinconichthys* might be united by a form of prognathy, with the mandibular symphysis extending beyond the anterior tip of the rostrodermethmoid. We are not convinced that life positions of these structures can be meaningfully assessed in available material of *Martillichthys* and *Rhinconichthys*, as at least some of the apparent prognathy of flattened specimens of these genera may be a result of taphonomic distortion rather than genuine anatomical signal. Second, we note the presence of a supraorbital canal-bearing rostrodermethmoid in *Martillichthys*, seen elsewhere in *Bonnerichthys* (Friedman *et al.* 2010). Although this arrangement is clearly derived relative to outgroups, the rostrodermethmoid of other edentulous pachycormiforms is insufficiently known to evaluate conditions in those taxa. Conclusions about the phylogenetic relevance of this character awaits additional study of relevant specimens or discovery of more satisfactory material. In summary, we argue that among well-known edentulous pachycormiforms, there appears to be strong support for a close relationship between *Asthenocormus* and *Martillichthys*, with *Rhinconichthys* and *Bonnerichthys* representing more distal outgroups to these sister genera.

Phylogenetic placement of poorly known taxa. *Ohmdenia* and *Leedsichthys* are two poorly known taxa that are, despite their incompleteness, particularly relevant to understanding the evolution of suspension-feeding pachycormiforms. The Early Jurassic *Ohmdenia*, with its unusual mandibular proportions and dentition, has been placed as the immediate sister lineage to edentulous pachycormiforms (Friedman 2012*a*; Schumacher *et al.* 2016), and thus has a bearing on primitive anatomical conditions of the clade. The Middle-Late Jurassic *Leedsichthys* is probably represented by the greatest amount of fossil material known for any edentulous pachycormiform (Liston 2010), but these remains are often difficult to interpret because of disarticulation and the damage to individual elements, as well as the difficulties posed in handling such quantities of

physically large material (Hudson & Martill 1994; Liston 2004; Liston 2016). Nevertheless, *Leedsichthys* has become perhaps the most iconic member of this radiation due to a combination of its great size and anatomical peculiarities (Liston 2004; Liston 2006; Liston *et al.* 2013; Liston 2016).

Ohmdenia, represented by a single associated but badly disrupted individual, presents an unusual combination of characters. It has proportionally elongate mandibles with a distinctive dentition comprising closely-packed, low-crowned teeth in broad bands across the dorsal margin of the mandible. Friedman (2012*a*) interpreted *Ohmdenia* as the sister lineage of edentulous pachycormiforms on the basis of two unambiguously optimized synapomorphies: the presence of a slab-sided hyomandibula and the apparent absence of scales. However, the phylogenetic hypothesis presented by Friedman (2012*a*) requires reversal to a more conventionally 'waisted' hyomandibula in *Martillichthys*, *Leedsichthys*, and *Asthenocormus*, raising questions about the reliability of this qualitative character. Unfortunately, many key aspects of anatomy with a bearing on placement of this taxon, including much of the skull, remain unknown. Intriguingly, the bone interpreted as the hyomandibula in *Ohmdenia* is very short in comparison to the mandible, broadly corresponding to conditions in *Asthenocormus* and *Martillichthys* rather than the more generalized pachycormiform proportions characteristic of *Bonnerichthys* and *Rhinconichthys* (Fig. 11). Additionally, the presumed hyomandibula appears to lack an opercular process, matching the condition reported in *Rhinconichthys* and *Asthenocormus*. Possible implications of this pattern are considered in the following section, but these hinge upon the uncertain identification of the hyomandibula in *Ohmdenia*.

Leedsichthys, although poorly known, shows some morphological features that support its phylogenetic placement among more completely known edentulous pachycormiforms. First, it possesses elongated gill rakers with oblique edges or fimbriations (Liston 2006, figs. 6.1-6.7; Gouiric-Cavalli 2017, fig. 2). Gill raker anatomy is known for some toothed pachycormiforms such as *Pachycormus* (BRLSI M1297; BRLSI M1361a, pers. obs.), which has small, knob-like rakers that are substantially shorter than the thickness of the supporting bones of the gill arches. These proportions are not dissimilar to what is seen in *Amia* (Grande &

Bemis 1998, fig. 56) and other outgroups, and we regard this as the primitive pachycormiform condition. By contrast, gill rakers are relatively elongate in *Martillichthys*, exceeding the thickness of their supporting gill bones. As very few individual rakers have been described in edentulous pachycormiforms, it is unclear how much they vary within and between individuals and species, limiting inferences made on the basis of observed morphological differences. The only edentulous pachycormiform not known to have elongated rakers is *Bonnerichthys*, which is regarded by this and most other studies as the sister lineage to all remaining edentulous pachycormiforms (Friedman *et al.* 2010; Friedman 2012*a*; Wretman *et al.* 2016). This stands in contrast to the sister group relationship between *Bonnerichthys* and *Leedsichthys* proposed by Schumacher *et al.* (2016, fig. 10). These authors do not report character optimizations for their preferred tree, but propose a lack of connections between the bones of the skull as a synapomorphy of these two genera. While the condition in *Bonnerichthys* is clear, we regard the structure of the skull in *Leedsichthys* as too poorly-known to assess this character, and maintain the hypothesis that *Bonnerichthys* is the sister taxon of all remaining edentulous pachycormiforms. The most informative material described for *Leedsichthys* is the gill basket NHMUK PV P.10156 (Liston 2008*a*, fig. 7; Liston *et al.* 2013, fig. 4), but the overall structure appears conservative, in line with accounts given for *Pachycormus* (Mainwaring 1978). The hyomandibula of *Leedsichthys* presents two relevant characters. First, it appears to lack an opercular process as in *Rhinconichthys* and (possibly) *Asthenocormus*, although it is possible that the process could have been damaged or lost in available material (cf. *Martillichthys*). Second, and perhaps more informatively, the hyomandibula is short in comparison to components of the ventral gill skeleton relative to the more generalized conditions in *Pachycormus* (Mainwaring 1978, figs. 11-12; pers. obs. CT scans of BRLSI M1297) and *Bonnerichthys* (Friedman *et al.* 2010, figs. 2, S7). This suggests that the hyomandibula was also short in comparison to the length of the lower jaw, which can be roughly approximated by the length of the first ventral gill arch. However, the condition in *Leedsichthys* does not appear as extreme as in *Martillichthys* and *Asthenocormus*. Although the illustration of the hyomandibula in *Asthenocormus* given in Lambers (1992, fig. 1*a*) is rudimentary, we are confident that the bone was relatively short given overall cranial geometry, even if more detailed aspects of its anatomy are unclear.

Implications for the evolution and ecology of edentulous pachycormiforms

Previous phylogenetic hypotheses (Friedman *et al.* 2010; Friedman 2012*a*), as well as the arrangement proposed here (Fig. 11), highlight some important questions about the evolution of edentulous pachycormiforms. One striking pattern to emerge from these studies is a general incongruence with stratigraphy. The most nested clade of edentulous pachycormiforms—comprising *Asthenocormus*, *Martillichthys*, and probably *Leedsichthys*—is Middle-Late Jurassic in age, and contains the oldest well-known edentulous pachycormiforms. Older material from the Bajocian is too incomplete to identify more precisely than a member of the edentulous pachycormiform clade (Friedman *et al.* 2010; Liston & Gendry 2015). By contrast, the Late Cretaceous *Bonnerichthys* and *Rhinconichthys* belong to earlier-diverging lineages, implying that each has a long unsampled history ranging from Middle Jurassic to Early Cretaceous - an interval of more than 60 million years. Although substantial, such a gap is not entirely unexpected; few diverse faunas of fully marine fishes are known from the Early Cretaceous, and, of these, the edentulous pachycormiforms are particularly rare. Instead, the most diverse fish localities known from this interval are largely freshwater (e.g. Las Hoyas, Sanz *et al.* 1988) or of mixed influence (e.g. Santana Formation; Martill 2007), with the few rich, but arguably understudied, marine fish faunas concentrated at the very end of the Early Cretaceous (e.g. Toolebuc Formation, Clode 2015; Gault Clay Formation, Forey & Longbottom 2010; Tlayúa Quarry, González-Rodríguez *et al.* 2013). In terms of overall cranial geometry, Late Cretaceous members of these early-diverging edentulous lineages do not closely resemble either well-known Late Jurassic taxa or the putative Early Jurassic sister-group of suspension-feeding pachycormiforms, *Ohmdenia*, all of which appear to have relatively narrow crania with deep suspensoria. By contrast, *Rhinconichthys* and *Bonnerichthys* have skull proportions that more closely resemble those of tooth-bearing pachycormiforms like *Pachycormus*. This hints at possibilities of a more complex evolutionary history of suspension-feeding pachycormiforms that should be tested by more detailed study of key taxa and revised phylogenetic analyses incorporating new anatomical observations.

In particular, *Bonnerichthys* presents a curious combination of characters relative to other edentulous pachycormiforms. Gill rakers are not known for this taxon despite nearly complete but disarticulated branchial arches, and an opercular process of the hyomandibula is retained; the latter feature is only known in *Martillichthys* among edentulous taxa, and even appears to be lost in *Ohmdenia*. Among edentulous pachycormiforms for which the condition can be assessed, *Bonnerichthys* is also an outlier in retaining a primitive geometry of the occiput. Set against these primitive features are peculiar derived traits of *Bonnerichthys* unique to that genus or otherwise only known in pachycormiforms in apparently distantly-related lineages. Among the latter, the most striking is distal fusion of individual lepidotrichia along the leading edges of the fin, which is characteristic of *Protosphyraena* (Dollo 1893; Friedman 2012*b*) and its probable junior synonym *Australopachycormus* (not reported in original description by Kear *et al.* 2007, but apparent in undescribed pectoral fin NHMUK PV P73611, also from the Toolebuc Formation of Australia and presumably attributable to the genus). This peculiar arrangement is regarded as convergent between the two groups, and is known to occur sporadically among other pachycormiforms (e.g. an isolated caudal fin from the Toarcian Beacon Limestone Formation of Strawberry Bank, UK, BRLSI M1393, likely attributable to *Pachycormus*). Such an incongruous distribution of characters raises some questions concerning the strength of support for the edentulous pachycormiform clade; many of the characters uniting these taxa relate to modifications associated with suspension-feeding, and therefore might not be independent of each other. Critical appraisal of the evolutionary history of edentulous pachycormiforms will also require a more detailed understanding of the anatomy of toothed members of the broader pachycormiform radiation. Although the balance of evidence at present appears to support the monophyly of edentulous pachycormiforms, we provide past studies of suspension-feeding lamniform sharks as a cautionary note. Early morphological studies of *Megachasma* argued for a sister-group relationship between this genus and *Cetorhinus*, with much of the supporting evidence deriving from anatomical features plausibly linked to suspension-feeding (Maisey 1985). Subsequent studies, including molecular analyses, reject the sister group relationship between cetorhinids and megachasmids (Martin & Naylor 1997; Motta 2004), but highlight the challenges presented by convergence upon broadly similar feeding modes by closely-related lineages.

Regardless of the phylogenetic implications of structural variations across edentulous pachycormiforms, it seems probable that major differences in head proportions point to important—but as yet undetermined—differences in feeding ecology. Cranial patterns among edentulous pachycormiforms range from the long, slender heads of *Martillichthys* and *Asthenocormus*, to the conventionally-proportioned head of *Rhinconichthys* associated with a slender hyomandibula, to the stout, large-eyed head of *Bonnerichthys*. Among living suspension feeders, the considerable variation in skull shape in closely related lineages appears linked to differences in feeding mode. Mysticete whales show substantial differences in overall cranial geometry (Sanderson & Wassersug 1993; Hampe & Baszio 2010), with morphologically distinctive lineages characterized by particular feeding modes: benthic suction feeding in grey whales (Eschrichtiidae); continuous ram feeding in bowhead and right whales (Balaenidae); and ram feeding in rorqual whales (Balaenopteridae; Goldbogen *et al.* 2007). Likewise, the independent radiations of mobuild, rhincodontid, megachasmid, and cetorhinid chondrichthyans have contrasting skull geometries associated with divergent approaches to suspension feeding (Moss 1977; Compagno 1990' Motta 2004; Motta *et al.* 2010; Paig-Tran & Summers 2014). It seems possible that the variation in cranial shape apparent in the suspension-feeding pachycormiforms could have some bearing on their feeding mechanisms. However, current treatments of the paleoecology of edentulous pachycormiforms are either quantitative but coarse (e.g. Friedman 2012*a*) or qualitative and limited to specific taxa (e.g. Schumacher *et al.* 2016), limiting any further inferences or comparisons to patterns of variation in living taxa. Additional information on the cranial anatomy of edentulous pachycormiforms will also help to better establish ecological diversity within this assemblage.

Conclusions

Re-examination of the skull of the Middle Jurassic (Callovian) *Martillichthys renwickae*, combined with μCT examination of previously concealed morphology, provides the most detailed account of cranial structure in edentulous pachycormiforms. This group has attracted considerable paleobiological and paleoecological interest, but even major aspects of their anatomy remain poorly understood for most of its

members. Reinterpretation of external details of the skull, including the snout, skull roof, cheek, lower jaw, operculogular series, and ventral hyoid arch brings the anatomy of *Martillichthys* more into line with conditions described in other pachycormiforms. μCT scanning reveals a premaxilla, portions of the braincase including a long, trough-like occipital stalk, a parasphenoid with a broad, paddle-like corpus, and an intact branchial skeleton. The latter preserves numerous club-shaped rakers, each bearing elongate, pointed projections. These rakers are found *in situ*, as with the gill basket specimen of *Leedsichthys*, representing the most complete picture yet available of the deployment of rakers across the gill skeleton in an edentulous pachycormiform.

Collectively, these observations reinforce past interpretations of *Martillichthys* as highly nested within the monophyletic edentulous pachycormiforms. In particular, the unusual cranial geometry of *Martillichthys*, characterized by a greatly elongated preorbital region of the skull and short hyomandibula, strongly supports a close relationship with the Late Jurassic *Asthenocormus*. Long ghost lineages leading to the Late Cretaceous *Rhinconichthys* and *Bonnerichthys* are inferred here as in most other studies of edentulous pachycormiforms. This is consistent with a poor Early Cretaceous record of marine fishes. However, the very generalized morphology of *Bonnerichthys* compared to both other edentulous pachycormiforms and the Early Jurassic *Ohmdenia* remains striking, and suggests that more exhaustive phylogenetic analyses of the group are necessary following more comprehensive documentation of anatomy in major pachycormiform lineages. Regardless of their exact patterns of interrelationships, a diversity of cranial geometries in edentulous pachycormiforms suggests a diversity of suspension-feeding strategies in this group, consistent with modern mysticete whales and planktivorous chondrichthyans.

Acknowledgements

We would like to thank Emma Bernard (NHM Earth Sciences) for access to the fossil fish collection, and Farah Ahmed and Amin Garbout (NHM Image and Analysis Centre) for access to the CT-scanning facilities.

We also thank Harry Taylor (NHM Photography Studio and Picture Library) for providing macrophotographs of NHMUK PV P.61563P. We thank Adriana López-Arbarello and an anonymous referee for their helpful comments on an earlier version of the manuscript. CD and MF were supported a Leverhulme Research Project Grant (RPG-2015-126). SG was supported by a Royal Society Dorothy Hodgkin Research Fellowship and a Junior Research Fellowship from Christ Church, Oxford.

Data Archiving Statement

Data for this study, including the raw scan data (TIFF stack), Mimics file, and three-dimension surface files (.ply) are available in the Dryad Digital Repository: https://datadryad.org/review?doi=doi:10.5061/dryad.XXXX

REFERENCES

ABRAMOFF, M. D., MAGALHAES, P. J. and RAM, S. J. 2004. Image Processing with ImageJ. *Biophotonics International*, **11**, 36–42.

ARRATIA, G. 2004. Mesozoic halecostomes and the early radiation of teleosts. 279–315. *In* ARRATIA, G. and TINTORI, A. (eds). *Mesozoic Fishes 3 - Systematics, Paleoenvironments and Biodiversity*. Verlag Dr Friedrich Pfeil, Münich, Germany, 649 pp.

—— and LAMBERS, P. 1996. The caudal skeleton of pachycormiforms. Parallel evolution? 191-218. *In* ARRATIA, G. and VIOHL, G. (eds). *Mesozoic Fishes 1 – Systematics and Paleoecology*. Verlag Dr Friedrich Pfeil, Münich, Germany, 576 pp.

—— and SCHULTZE, H. P. 2013. Outstanding features of a new Late Jurassic pachycormiform fish from the Kimmeridgian of Brunn, Germany and comments on current understanding of pachycormiforms. 87-120. *In* ARRATIA, G., SCHULTZE, H. P. and WILSON, M. V. H. (eds). *Mesozoic Fishes 5 – Global Diversity and Evolution*. Verlag Dr Friedrich Pfeil, Münich, Germany, 560 pp.

BARTHEL, K. W., SWINBURNE, N. H. M. and MORRIS, S. C. 1990. *Solnhofen: A Study in Mesozoic Palaeontology.* Cambridge University Press, Cambridge, 236 pp.

BELLWOOD, D. R. 2003. Origins and escalation of herbivory in fishes: a functional perspective. *Paleobiology*, **29**, 71–83.

BERG, L. S. 1937. A classification of fish-like vertebrates. *Bulletin de l'Académie des Sciences de l'URSS*, **4**, 1277–1280.

CAWLEY, J. J., KRIWET, J., KLUG, S. and BENTON, M. J. 2018. The stem group teleost *Pachycormus* (Pachycormiformes: Pachycormidae) from the Upper Lias (Lower Jurassic) of Strawberry Bank, UK. *Paläontologische Zeitschrift*, 1-18.

CIONE, A. L., SANTILLANA, S., GOUIRIC-CAVALLI, S., HOSPITALECHE, C. A., GELFO, J. N., LÓPEZ, G. M. and REGUERO, M. 2018. Before and after the K/Pg extinction in West Antarctica: New

marine fish records from Marambio (Seymour) Island. *Cretaceous Research*, published online 2 February 2018. doi:10.1016/j.cretres.2018.01.004

CLODE, D. 2015. *Prehistoric Marine Life in Australia's Inland Sea*. Museum Victoria, Melbourne, 84 pp.

COPE, E. D. 1887. Zittel's Manual of Palaeontology. *American Naturalist*, **17**, 1014–1019.

CUNNINGHAM, J. A., RAHMAN, I. A., LAUTENSCHLAGER, S., RAYFIELD, E. J. and DONOGHUE, P. C. 2014. A virtual world of palaeontology. *Trends in Ecology and Evolution*, **29**, 347–357.

DOLLO, L. 1893. Nouvelle note sur les poissons de la Craie phosphatée. *Bulletin de la Société belge de Géologie, de Paléontologie et d'Hydrologie*, **7**, 180-189.

EITING, T. P. and SMITH, G. R. 2007. Miocene salmon (*Oncorhynchus*) from Western North America: Gill raker evolution correlated with plankton productivity in the Eastern Pacific. *Palaeogeography, Palaeoclimatology, Palaeoecology*, **249**, 412–424.

FELIX, J. 1890. Beiträge zur Kenntniss der Gattung *Protosphyraena* Leidy. *Deutsche Geologische Gesellschaft, Berlin Zeitschrift*, **42**, 278-302.

FERRÓN, H. G., HOLGADO, B., LISTON, J. J., MARTINEZ-PEREZ, C., and BOTELLA, H. 2018. Assessing metabolic constraints on the maximum body size of actinopterygians: locomotion energetics of *Leedsichthys problematicus* (Actinopterygii, Pachycormiformes). *Palaeontology*, **61**, 775–783.

FOREY, P. L. and LONGBOTTOM, A. 2010. Bony fishes. 261–269. *In* YOUNG, J. R., GALE, A. S., KNIGHT, R. I. and SMITH, A. B. (eds). *Fossils of the Gault Clay*. Palaeontological Association, Field Guides to Fossils, **12**, 342 pp.

FRIEDMAN, M. 2012*a*. Parallel evolutionary trajectories underlie the origin of giant suspension-feeding whales and bony fishes. *Proceedings of the Royal Society of London B: Biological Sciences*, **279**, 944–951.

—— 2012*b*. Ray-finned fishes (Osteichthyes, Actinopterygii) from the type Maastrichtian, the Netherlands and Belgium. *Scripta Geologica Special Issue*, **8**, 113–142.

—— SHIMADA, K., MARTIN, L. D., EVERHART, M. J., LISTON, J., MALTESE, A. and TRIEBOLD, M. 2010. 100-million-year dynasty of giant planktivorous bony fishes in the Mesozoic seas. *Science*, **327**, 990–993.

—— —— EVERHART, M. J., IRWIN, K. J., GRANDSTAFF, B. S. and STEWART, J. D. 2013. Geographic and stratigraphic distribution of the Late Cretaceous suspension-feeding bony fish *Bonnerichthys gladius* (Teleostei, Pachycormiformes). *Journal of Vertebrate Paleontology*, **33**, 35–47.

GARDINER, B. G. and SCHAEFFER, B. 1989. Interrelationships of lower actinopterygian fishes. *Zoological Journal of the Linnaean Society*, **97**, 135–187.

—— —— and MASSERIE, J. A. 2005. A review of the lower actinopterygian phylogeny. *Zoological Journal of the Linnaean Society*, **144**, 511–525.

GILES, S., ROGERS, M. and FRIEDMAN, M. 2016. Bony labyrinth morphology in early neopterygian fishes (Actinopterygii: neopterygii). *Journal of Morphology*, **279**, 426-440.

GOLDBOGEN, J. A., PYENSON, N. D. and SHADWICK, R. E. 2007. Big gulps require high drag for fin whale lunge feeding. *Marine Ecology Progress Series*, **349**, 289-301.

GONZÁLEZ-RODRÍGUEZ, K. A., ESPINOZA-ARRUBARRENA, L. and GONZÁLEZ-BARBA, G. 2013. An overview of the Mexican fish fossil record. 9–34. *In* ARRATIA, G., SCHULTZE, H. P. and WILSON, M. V. H. (eds). *Mesozoic Fishes 5 – Global Diversity and Evolution*. Verlag Dr Friedrich Pfeil, Münich, Germany, 560 pp.

GOUIRIC-CAVALLI, S. 2013. Sistemática y relaciones biogeográficas de los peces del Titoniano (Jurásico tardío) de la Cuenca Neuquina de Argentina. Unpublished PhD thesis, Universidad Nacional de La Plata, La Plata, 583 pp.

—— 2017. Large and mainly unnoticed: the first Lower Tithonian record of a suspension-feeding pachycormid from southern Gondwana. *Ameghiniana*, **54**, 283–289.

—— and CIONE, A. L. 2015. *Notodectes* is the first endemic pachycormiform genus (Osteichthyes, Actinopterygii, Pachycormiformes) in the Southern Hemisphere. *Journal of Vertebrate Paleontology*, **35**, e933738-1–e933738-11.

—— RASIA, L. L., MÁRQUEZ, G. J., ROSATO, V., SCASSO, R. A. and REGUERO, M. in press. First pachycormiform (Actinopterygii, Pachycormiformes) remains from the Late Jurassic of the Antarctic Peninsula and remarks on bone alteration by recent bioeroders. *Journal of Vertebrate Paleontology*, **38**.

GRADSTEIN, F. M. E., OGG, J. G., SCHMITZ, M. D. and OGG, G. M. 2012. *The Geologic Time Scale 2012*, Elsevier, Amsterdam, 1140 pp.

GRANDE, L. 2010. An empirical synthetic pattern study of gars (Lepisosteiformes) and closely related species, based mostly on skeletal anatomy. The resurrection of Holostei. Copeia, 10, 1–863.

—— and BEMIS, W. E. 1998. A comprehensive phylogenetic study of amiid fishes (Amiidae) based on comparative skeletal anatomy. An empirical search for interconnected patterns of natural history. *Society of Vertebrate Paleontology, Memoir*, **4**, 1–690.

HAIG, D. W. 1979. Cretaceous foraminiferal biostratigraphy of Queensland. *Alcheringa*, **3**, 171-187.

HAMPE, O. and BASZIO, S. 2010. Relative warps meet cladistics: A contribution to the phylogenetic relationships of baleen whales based on landmark analyses of mysticete crania. *Bulletin of Geosciences*, **85**, 199-218.

HAUFF, B. 1953. *Das Holzmadenbuch*. Hohenlohe'sche Buchhandlung Ferdinand Rau, Öhringen, Germany, 134 pp.

HAY, O. P. 1903. On certain genera and species of North American Cretaceous actinopterous fishes. *Bulletin of the American Museum of Natural History*, **91**, 1–95.

HUDSON, J. D. and MARTILL, D. M. 1994. The Peterborough Member (Callovian, Middle Jurassic) of the Oxford Clay Formation at Peterborough, UK. *Journal of the Geological Society*, **151**, 113-124.

KEAR, B. P. 2007. First record of pachycormid fish (Actinopterygii: Pachycormiformes) from the Lower Cretaceous of Australia. *Journal of Vertebrate Palaeontology*, **27**, 1033–1038.

LAMBERS, P. H. 1988. *Orthocormus teyleri* nov. spec., the first pachycormid (Pisces, Actinopterygii) from the Kimmeridge [sic] Lithographic Limestone at Cerin (Ain), France; with remarks on the genus *Orthocormus* Weitzel. *Proceedings of the Koninklijke Nederlandse Akademie van Wetenschappen Series B*, **91**, 369–391.

—— 1992. On the ichthyofauna of the Solnhofen Lithographic Limestone (Upper Jurassic, Germany). Unpublished PhD thesis, Rijkuniversiteit Groningen, Groningen, 336 pp.

LEHMAN, J. P. 1949. Étude d'un *Pachycormus* du Lias de Normandie. *Kungliga Svenska Vetenskapsakademiens Handlingar*, **4**, 1–44.

LISTON, J. 2006. A fish fit for Ozymandias?: the ecology, growth and osteology of *Leedsichthys* (Pachycormidae, Actinopterygii). Unpublished PhD thesis, University of Glasgow, Glasgow, 464 pp.

—— 2008*a*. A review of the characters of the edentulous pachycormiforms *Leedsichthys*, *Asthenocormus* and *Martillichthys* nov. gen. 181–198. *In* ARRATIA, G., SCHULTZE, H. P. and WILSON, M. V. H. (eds). *Mesozoic Fishes 4 – Homology and Phylogeny.* Verlag Dr Friedrich Pfeil, Münich, Germany, 502 pp.

—— 2008*b*. *Leedsichthys* des Vaches Noires au peigne fin (translation by M-C Buchy). *L'Écho des Falaises*, **12**, 41-49.

—— 2010. The occurrence of the Middle Jurassic pachycormid fish *Leedsichthys*. *Oryctos*, **9**, 1-36.

—— 2013. The plasticity of gill raker characteristics in suspension feeders: implications for Pachycormiformes. 121–143. *In* ARRATIA, G., SCHULTZE, H. P. and WILSON, M. V. H. (eds). *Mesozoic Fishes 5 – Global Diversity and Evolution*. Verlag Dr Friedrich Pfeil, Münich, Germany, 560 pp.

—— 2016. *Leedsichthys problematicus*: Arthur Smith Woodward's 'most embarrassing enigma'. *Geological Society London: Special Publications*, **430**, 235–259.

—— and GENDRY, D. 2015. Le Python de Caen, les algues géantes d'Amblie, et autres specimens perdus de *Leedsichthys* d'Alexandre Bourienne, Jules Morière, Eugène Eudes-Deslongchamps et Alexandre Bigot. *L'Écho des Falaises*, **19**, 17-33.

—— and Maltese, A. 2016. Daggers, swords, scythes and sickles: Pachycormid fins as ecological predictors. *PeerJ Preprints*, **4**, e2550v1.

—— NEWBREY, M., CHALLANDS, T. and ADAMS, C. 2013. Growth, age and size of the Jurassic pachycormid *Leedsichthys problematicus* (Osteichthyes: Actinopterygii). 145–175. *In* ARRATIA, G.,

SCHULTZE, H. P. and WILSON, M. V. H. (eds). *Mesozoic Fishes 5 – Global Diversity and Evolution*. Verlag Dr Friedrich Pfeil, Münich, Germany, 560 pp.

LOOMIS, F. B. 1900. Die anatomie und die verwandtschaft der Ganoid- und Knochen-fische aus der Kreide-Formation von Kansas, U.S.A. *Paleontographica*, **46**, 213-283.

LÓPEZ-ARBARELLO, A. and SFERCO, E. 2018. Neopterygian phylogeny: the merger assay. *Royal Society Open Science*, **5**, 172337.

MAINWARING, A. J. 1978. Anatomical and systematic revision of the Pachycormidae, a family of Mesozoic fishes. Unpublished PhD thesis, Westfield College, London, 127 pp.

MAISEY, J. G. 1985. Relationships of the megamouth shark, Megachasma. *Copeia*, **1985**, 228-231.

MARTILL, D. M. 1986. The stratigraphic distribution and preservation of fossil vertebrates in the Oxford Clay of England. *Philosophical Transactions of the Royal Society of London B: Biological Sciences*, **311**, 155–165.

—— 1988. *Leedsichthys problematicus*, a giant filter-feeding teleost from the Jurassic of England and France. *Neues Jahrbuch fur Geologie und Palaontologie-Monatshefte*, **11**, 670–680.

—— 2007. The age of the Cretaceous Santana Formation fossil Konservat Lagerstätte of north-east Brazil: a historical review and an appraisal of the biochronostratigraphic utility of its palaeobiota. *Cretaceous Research*, **28**, 895-920.

—— 1991. Fish. 197-225. In MARTILL, D. M. and HUDSON, J. D. (eds). *Fossils of the Oxford Clay*. Palaeontological Association Field Guide to Fossils, **4**, The Palaeontological Association. 286 pp.

MARTIN, A. P. and NAYLOR, G. J. 1997. Independent origins of filter-feeding in megamouth and basking sharks (order Lamniformes) inferred from phylogenetic analysis of cytochrome *b* gene sequences. 39-50. *In* YANO, K., MORRISSEY, J. F., YABUMOTO, Y. and NAKAYA, K. (eds). *Biology of Megamouth Shark*. Tokai University Press, Tokyo, 203 pp.

McCLUNG, C. E. 1908. Ichthyological notes of the Kansas Cretaceous, I. *Kansas University Science Bulletin*, **9**, 235–246.

MOSS, S. 1977. Feeding mechanisms in sharks. *American Zoologist*, **17**, 355-364.

MOTTA, P. J. 2004. Prey capture behavior and feeding mechanics of elasmobranchs. 165-203. *In* CARRIER, J. C., MUSICK, J. A. and HEITHAUS, M. R. (eds). *Biology of Sharks and Their Relatives*. 2nd edn. CRC Press, Boca Raton, Florida, 666 pp.

MOTTA, P. J., MASLANKA, M., HUETER, R. E., DAVIS, R. L., DE LA PARRA, R., MULVANY, S. L., HABEGGER, M. L., STROTHER, J. A., MARA, K. R., GARDINER, J. M., TYMINSKI, J. P. and ZEIGLER, L. D. 2010. Feeding anatomy, filter-feeding rate, and diet of whale sharks *Rhincodon typus* during surface ram filter feeding off the Yucatan Peninsula, Mexico. *Zoology*, **113**, 199-212.

MÜLLER, J. 1845. Ueber den Bau und die Grenzen der Ganoiden und über das natürliche System der Fische. *Archiv für Naturgeschichte*, **11**, 91–141.

NELSON, G. 1969. Gill arches and the phylogeny of fishes, with notes on the classification of vertebrates. *Bulletin of the American Museum of Natural History*, **141**, 475–552.

OLSEN, P. E. 1984. The skull and pectoral girdle of the parasemionotid fish *Watsonulus eugnathoides* from the Early Triassic Sakamena Group of Madagascar, with comments on the relationships of the holostean fishes. *Journal of Vertebrate Paleontology*, **4**, 481–499.

PATTERSON, C. 1973. Interrelationships of holosteans. 233–305. *In* GREENWOOD, P. H., MILES, R. S. and PATTERSON, C. (eds). *Interrelationships of Fishes*, **53**, Academic Press, Cambridge, Massachusetts, 496 pp.

—— 1975. The braincase of pholidophorid and leptolepid fishes, with a review of the actinopterygian braincase. *Philosophical Transactions of the Royal Society of London B: Biological Sciences*, **269**, 275–579.

—— 1994. Bony fishes. *Short courses in Paleontology*, **7**, 57–84.

POPLIN, C. M. 1984. *Lawrenciella schaefferi* ng, n. sp. (Pisces: Actinopterygii) and the use of endocranial characters in the classification of the palaeonisciformes. *Journal of Vertebrate Paleontology*, **4**, 413–421.

QUENSTEDT, F. A. 1852. *Handbuch der Petrefactenkunde. Laupp'sche Buchhandlung*, Tübingen, Germany, 792 pp.

RAYNER, D. H. 1948. The structure of certain Jurassic holostean fishes, with special reference to their neurocrania. *Philosophical Transactions of the Royal Society of London B: Biological Sciences*, **233**, 287-345.

REGAN, C. T. 1923. The skeleton of *Lepidosteus*, with remarks on the origin and evolution of the lower neopterygian fishes. *Journal of Zoology*, **93**, 445–461.

SANDERSON, S. L. and WASSERSUG, R. 1993. Convergent and Alternative Designs for Vertebrate Suspension Feeding. 37–112. *In* HANKEN, J. and HALL, B. K. (eds). *The Skull: Volume 3*, University of Chicago Press, Chicago, Illinois, 470 pp.

SANSOM, R. S. 2014. Bias and sensitivity in the placement of fossil taxa resulting from interpretations of missing data. *Systematic Biology*, **64**, 256–266.

SANZ, J. L., WENZ, S., YEBENES, A., ESTES, R., MARTINEZ-DELCLOS, X., JIMENEZ-FUENTES, E., DIÉGUEZ, C., BUSCALIONI, A. D., BARBADILLO, L. J. and VIA, L. 1988. An Early Cretaceous faunal and floral continental assemblage: Las Hoyas fossil site (Cuenca, Spain). *Geobios*, **21**, 611-635.

SCHAEFFER, B. and PATTERSON, C. 1984. Jurassic fishes from the western United States, with comments on Jurassic fish distribution. *American Museum Noviates*, **2796**, 1–86.

—— and ——. 1990. Suspension-feeding vertebrates. *Scientific American*, **262**, 96-102.

SCHUMACHER, B. A., SHIMADA, K., LISTON, J. and MALTESE, A. 2016. Highly specialized suspension-feeding bony fish *Rhinconichthys* (Actinopterygii: Pachycormiformes) from the mid-Cretaceous of the United States, England, and Japan. *Cretaceous Research*, **61**, 71–85.

STEWART, J. D. 1988. The stratigraphic distribution of Late Cretaceous *Protosphyraena* in Kansas and Alabama. 80–94. *In* NELSON, M. E. (ed). *Paleontology and Biostratigraphy of Western Kansas*: *Articles in Honor of Myrl V. Walker*. Fort Hays Studies, **3**, Fort Hays State University, Kansas.

—— 1990. Niobrara formation vertebrate stratigraphy. 19–30. *In* BENNETT, S. C. (ed.), *Niobrara Chalk Excursion Guidebook*. Museum of Natural History and Kansas Geological Survey, Lawrence, Kansas.

SUTTON, M. D., BRIGGS, D. E., SIVETER, D. J. and SIVITER, D. J. 2001. Methodologies for the visualisation and reconstruction of three-dimensional fossils from the Silurian Herefordshire Lagerstätte. *Palaeontologia Electronica*, **4**, 1–17.

TAVERNE, L. and LISTON, J. 2017. On the presence of the plethodid fish *Dixonanogmius* (Teleostei, Tselfatiiformes) in the marine Upper Cretaceous of Burma (Myanmar), tropical Asia. *Geo-Eco-Trop*, **41**, 77-84.

WARD, D. J. and HOLLINGWORTH, N. T. 1990. The first record of a bitten ammonite from the Middle Oxford Clay (Callovian, Middle Jurassic) of Bletchley, Buckinghamshire. *Mesozoic Research*, **2**, 153–161.

WEITZEL, K. 1930. Drei Riesenfische aus den Solnhofener Schiefern von Langenaltheim. *Abhandlungen der Senckenbergischen Naturforschenden Gesellschaft*, **42**, 85–113.

WENZ, S. 1967. *Complements a Retude des Poissons Actinopterygiens du Jurassique Francaise*, Paris: Centre national de la Recherche Scientifique, 276 pp.

WILLIAMS, M., BENTON, M. J. and ROSS, A. 2015. The Strawberry Bank Lagerstätte reveals insights into Early Jurassic life. *Journal of the Geological Society*, **172**, 683–692.

WOODWARD, A. S. 1889*a*. On the palaeontology of sturgeons. *Proceedings of the Geologists' Association*, **11**, 24–44.

—— 1889*b*. Preliminary notes on some new and little-known British Jurassic fishes. *Geological Magazine*, **6**, 448–455.

—— 1895. *Catalogue of the Fossil Fishes in the British Museum,* **3**, British Museum (Natural History), London, 544 pp.

WRETMAN, L., BLOM, H. and KEAR, B. P. 2016. Resolution of the Early Jurassic actinopterygian fish *Pachycormus* and a dispersal hypothesis for Pachycormiformes. *Journal of Vertebrate Paleontology*, **36**, e1206022-1–e1206022-8.

FIGURE CAPTIONS

FIG. 1. Skull of *Martillichthys renwickae* NHMUK PV P.61563P. A, photograph in ventral view. B, photograph in dorsal view. Anterior to the left in panel A; and to the right in panel B. Scale bar represents 10 cm. *(intended for full page width)*

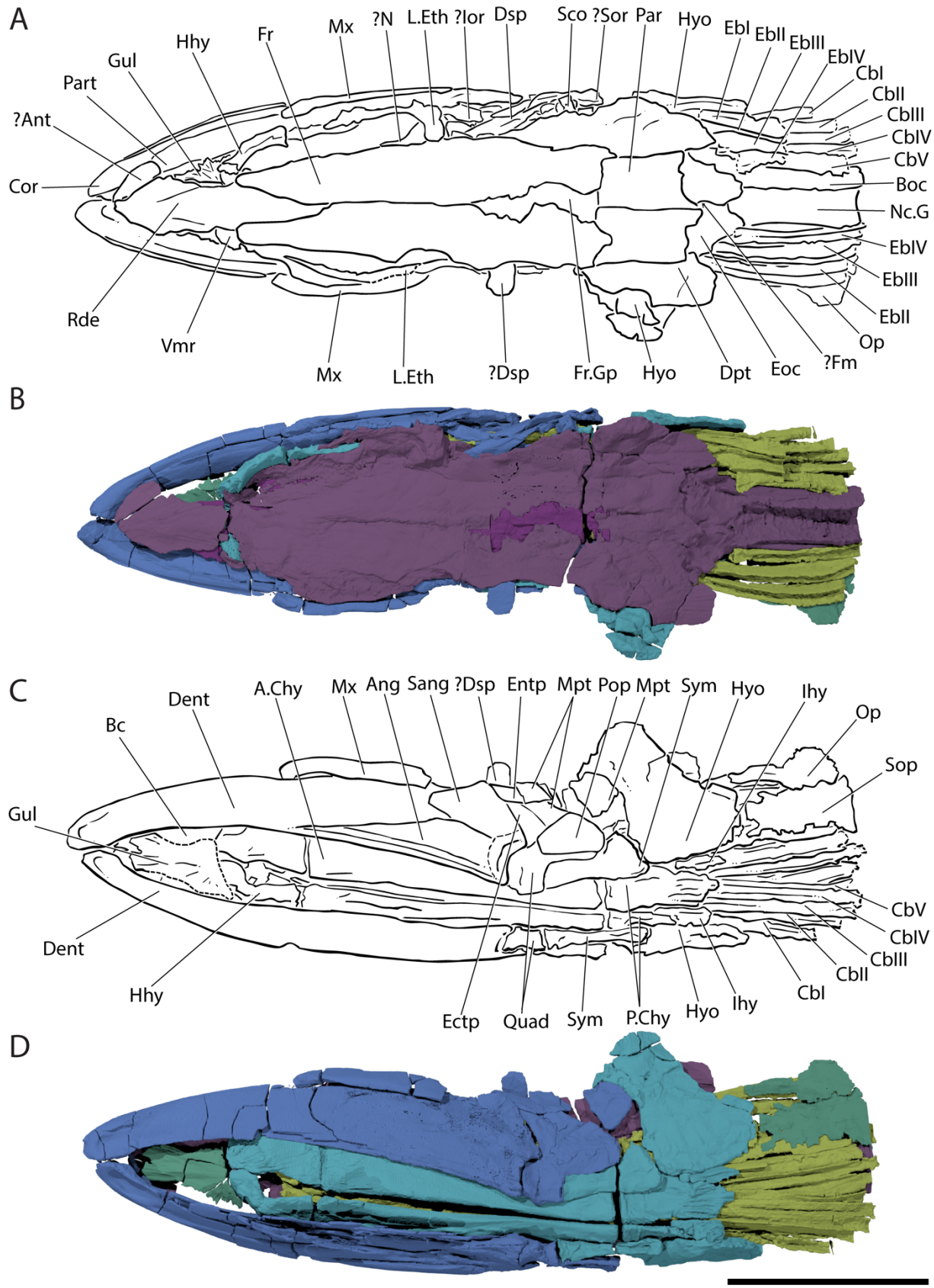

FIG. 2. Skull of *Martillichthys renwickae* NHMUK PV P.61563P. A, interpretive line drawing of rendered portions of the skull in dorsal view. B, three-dimensional rendering of skull in dorsal view. C, interpretive line drawing of rendered portions of the skull in ventral view. D, three-dimensional rendering of skull in

ventral view. Hashed lines indicate areas where margins are uncertain. *Abbreviations*: A.Chy, anterior ceratohyal; Ang, angular; ?Ant, antorbital; Bc, braincase; Boc, basioccipital; Cb, ceratobranchial; Cor, coronoid; Dent, dentary; Dpt, dermopterotic; Dsp, dermosphenotic; Ectp, ectopterygoid; Entp, entopterygoid; Eoc, exoccipital; Eb, epibranchial; ?Fm, foramen magnum; Fr, frontal; Fr.Gp; frontal gap; Gul, gular; Hhy, hypohyal; Hyo, hyomandibula; Ihy, interhyal; ?Ior, infraorbital; L.Eth, lateral ethmoid; Mpt, metapterygoid; Mx, maxilla; ?N, nasal; Nc.G, notochord groove; Op, operculum; Par, parietal; Part, prearticular; P.Chy, posterior ceratohyal; Pop, preoperculum; Quad, quadrate; Rde, rostrodermethmoid; Sang, surangular; Sco, sclerotic ossicle; Sop, suboperculum; ?Sor, suborbital; Sym, symplectic; Vmr, vomer. Anterior to the left. Scale bar represents 10 cm. *(intended for full page width)*

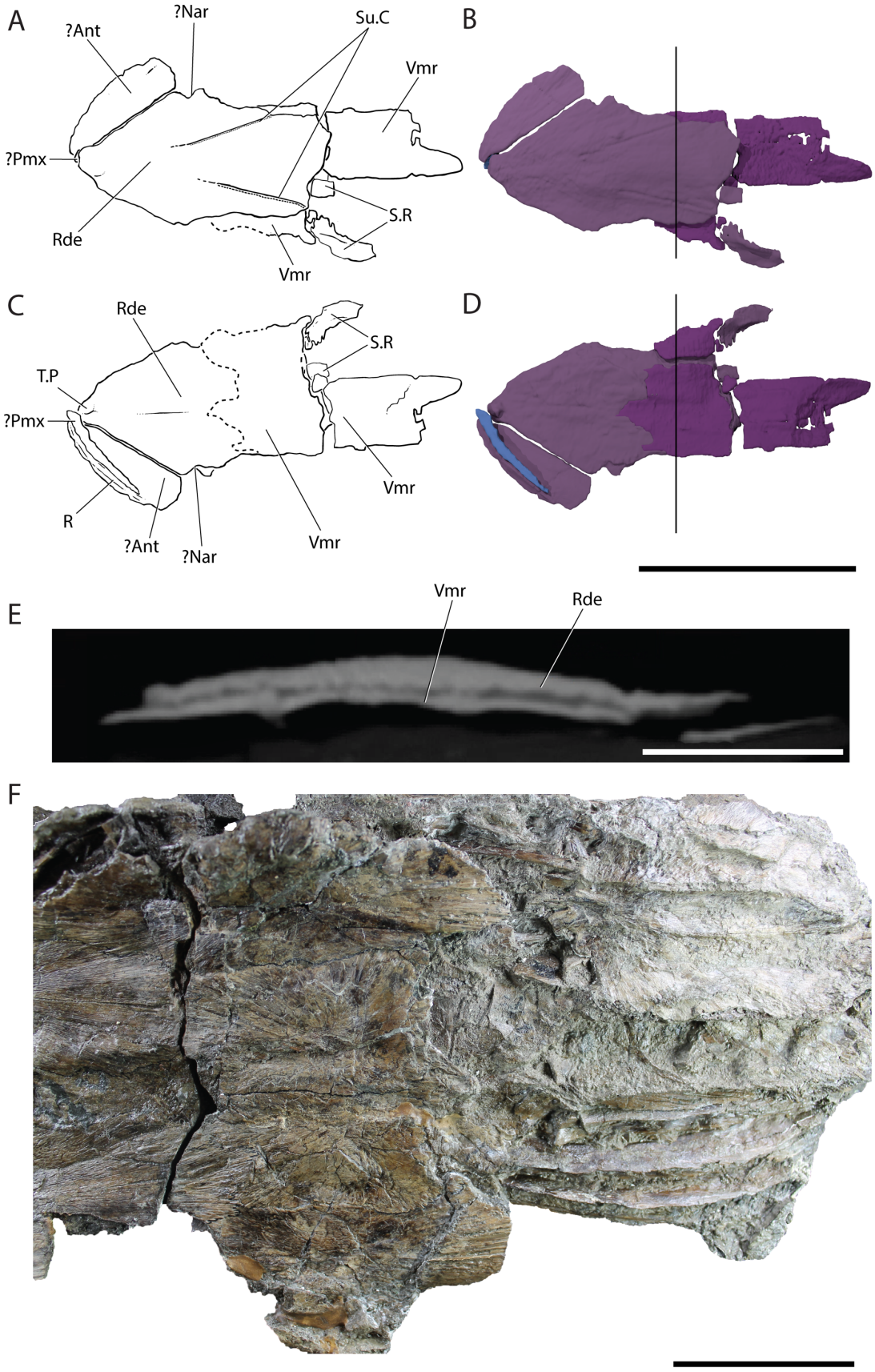

FIG. 3. Anterior portion of the rostrodermethmoid and putative vomer and antorbital of *Martillichthys renwickae*, NHMUK PV P.61563P. A, interpretive drawing in dorsal view. B, three-dimensional render in dorsal view. C, interpretive drawing in ventral view. D, three-dimensional render in ventral view. E,

transverse cross-section through rostrodermethmoid and vomer. F, photograph of the posterior half of the skull roof, and the exposed gill skeleton. Black line in panels B and D indicates position of panel E. Dashed lines indicate where margins are uncertain. Anterior to the left in panels A–D, F. *Abbreviations*: ?Ant, antorbital; ?Nar, naris; ?Pmx, premaxilla; R, ridge; Rde, rostrodermethmoid; ?Su.C, supraorbital canal; S.R, skull roofing bones; T.P, thickened portion; Vmr, vomer. Scale bar represents 5 cm. *(intended for full page width)*

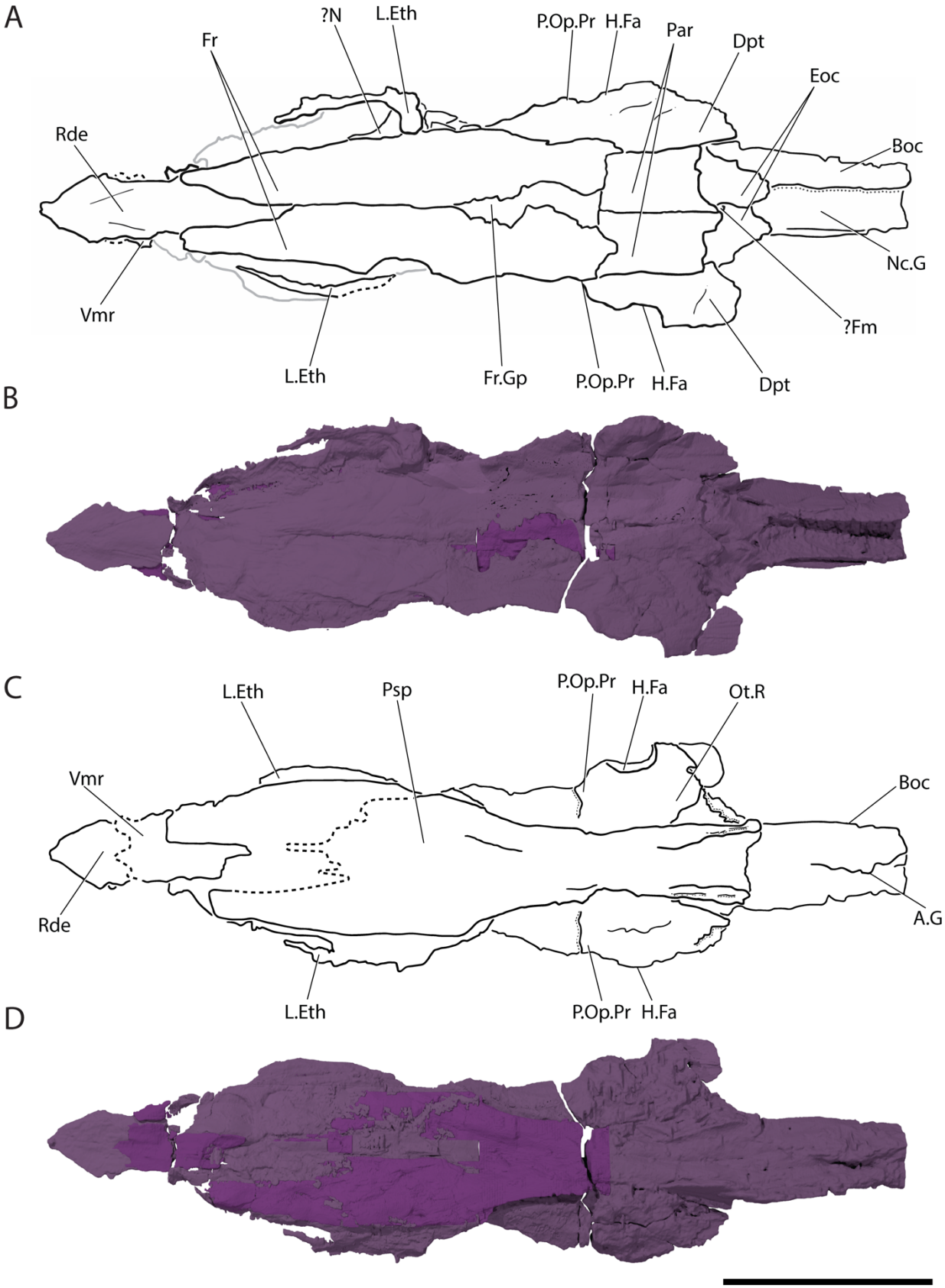

FIG. 4. Skull roof and braincase of *Martillichthys renwickae* NHMUK PV P.61563P. A, interpretive drawing in dorsal view. B, three-dimensional render in dorsal view. C, interpretive drawing in ventral view. D, three-dimensional render in ventral view. Grey lines represent undefined structures and surrounding matrix.

Dashed lines indicate areas where margins are uncertain. *Abbreviations*: A.G, aortic groove; Boc, basioccipital; Dpt, dermopterotic; Eoc, exoccipital; ?Fm, foramen magnum; Fr, frontal; Fr.Gp; frontal gap; H.Fa, hyoid facet; L.Eth, lateral ethmoid; ?N, nasal; Nc.G, notochord groove; Ot.R, otic region; Par, parietal; P.Op.Pr, postorbital process; Psp, parasphenoid; Rde, rostrodermethmoid; Vmr, vomer. Anterior to the left. Scale bar represents 10 cm for panels A–D and 2 cm for panel E. *(intended for full page width)*

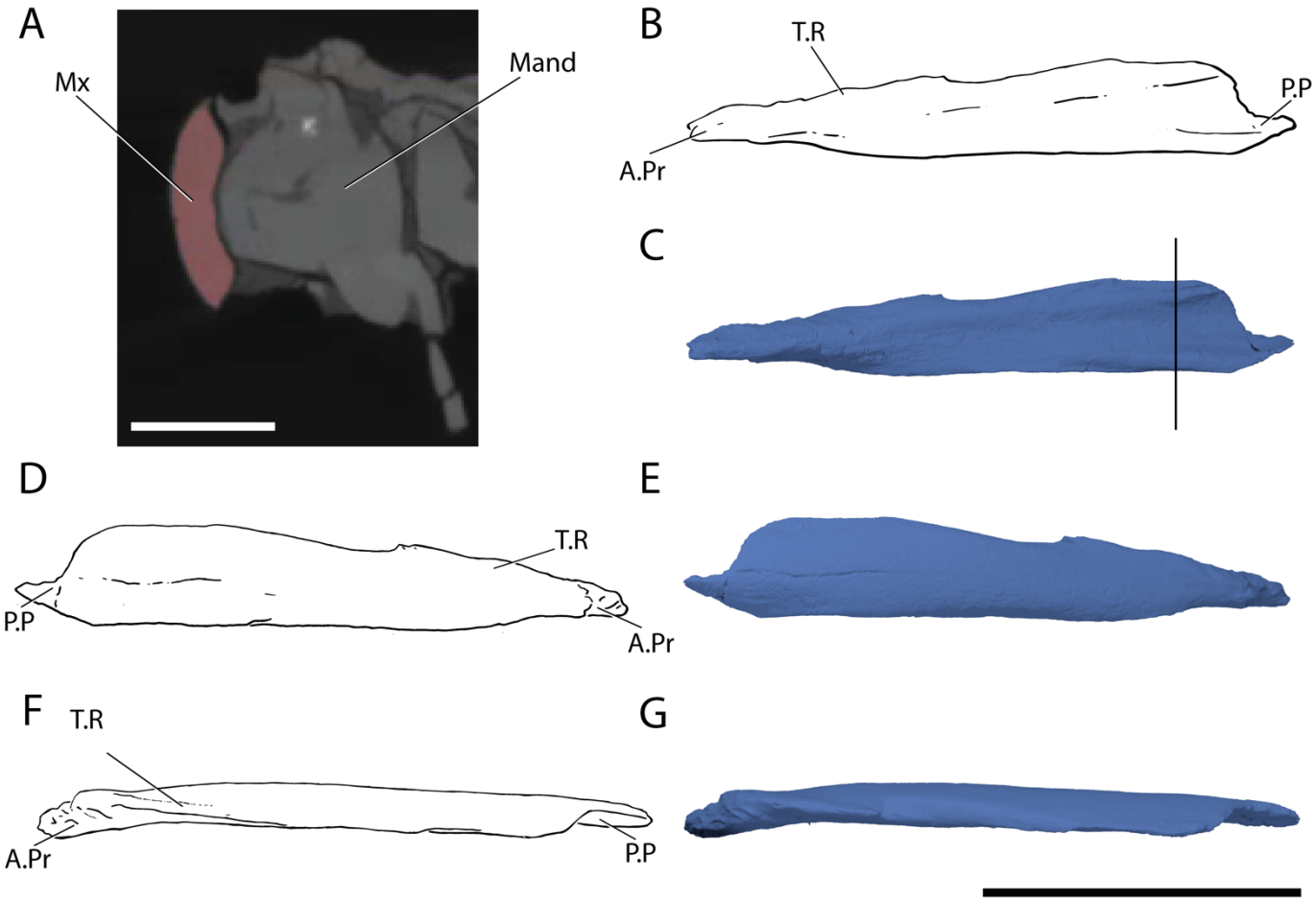

FIG. 5. Maxilla of *Martillichthys renwickae* NHMUK PV P.61563P. A, transverse cross-section through maxilla. B, interpretive drawing of left maxilla in mesial view. C, three-dimensional render of maxilla in mesial view. D, interpretive drawing of left maxilla in lateral view. E, three-dimensional render of left maxilla in lateral view. F, interpretive drawing of left maxilla in dorsal view. G, three-dimensional render of left maxilla in dorsal view. Black line in panel C indicates position of panel A. Anterior to the left in panels B, C, F and G, and to the right in D and E. *Abbreviations*: A.Pr, articular process; Mand, mandible; Mx, maxilla; P.P, posterior prong; T.R, thickened ridge. Scale represents 10 cm. *(intended for full page width)*

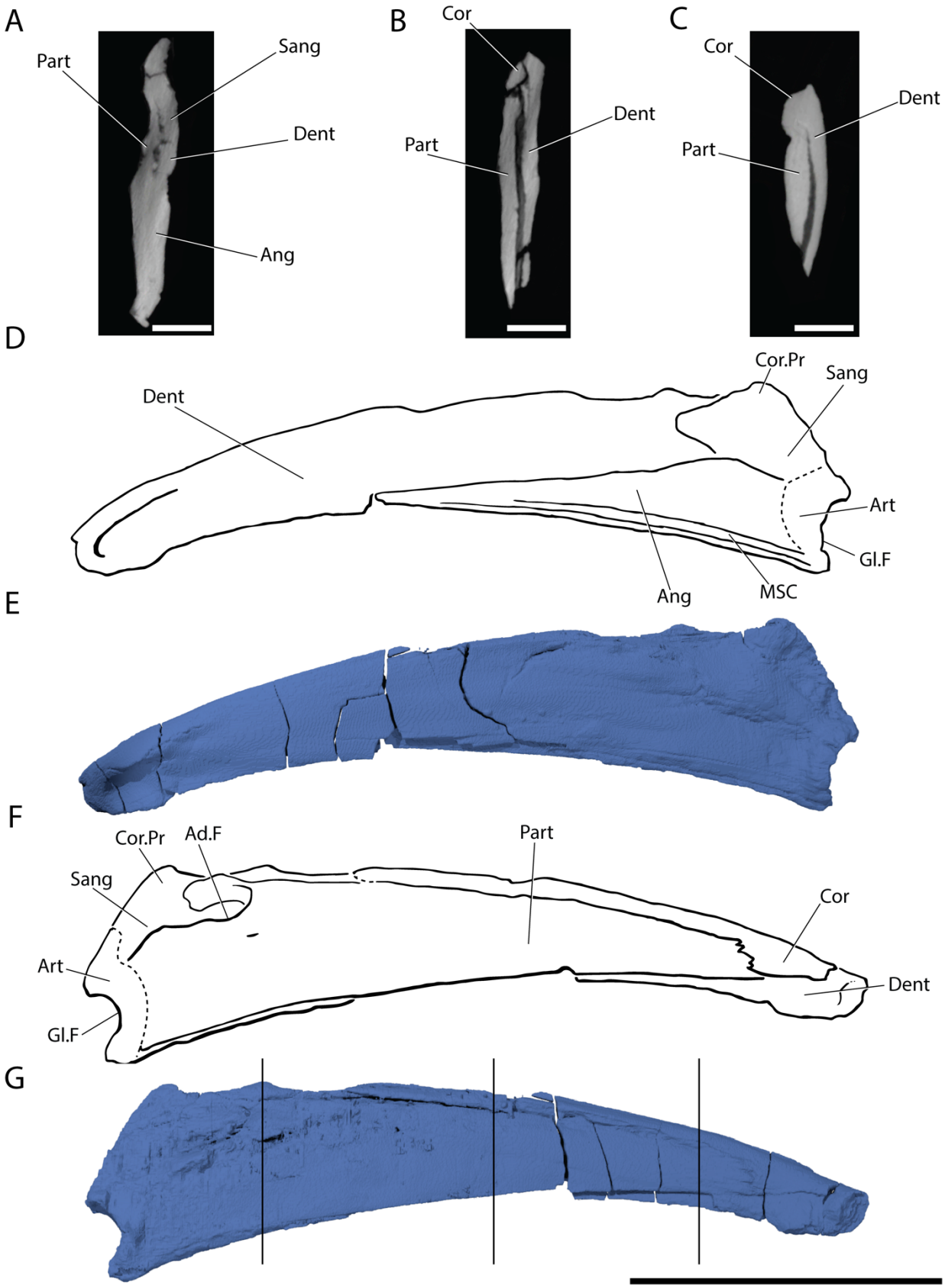

FIG. 6. Mandible of *Martillichthys renwickae* NHMUK PV P.61563P. A, transverse cross-section through mandible in the region of the adductor fossa. B, transverse cross-section through mandible at the approximate midpoint. C, transverse cross-section through mandible near anterior margin of coronoid. D, interpretive

drawing of left mandible in lateral view. E, three-dimensional render of left mandible in lateral view. F, interpretive drawing of left mandible in mesial view. G, three-dimensional render of left mandible in mesial view. Black lines in panel G indicate position of panels A, B and C from left to right. Anterior to the right in panels F and G; to the left in panels D and E. Dashed lines indicate areas where margins are uncertain. *Abbreviations*: Ad.F, adductor fossa; Ang, angular; Art, articular; Cor, coronoid; Cor.Pr, coronoid process; Dent; dentary; Gl.F, glenoid fossa; MSC, mandibular sensory canal; Part, prearticular; Sang, surangular. Scale in panels A-C represent 1 cm, and 10 cm in panels D-G. *(intended for full page width)*

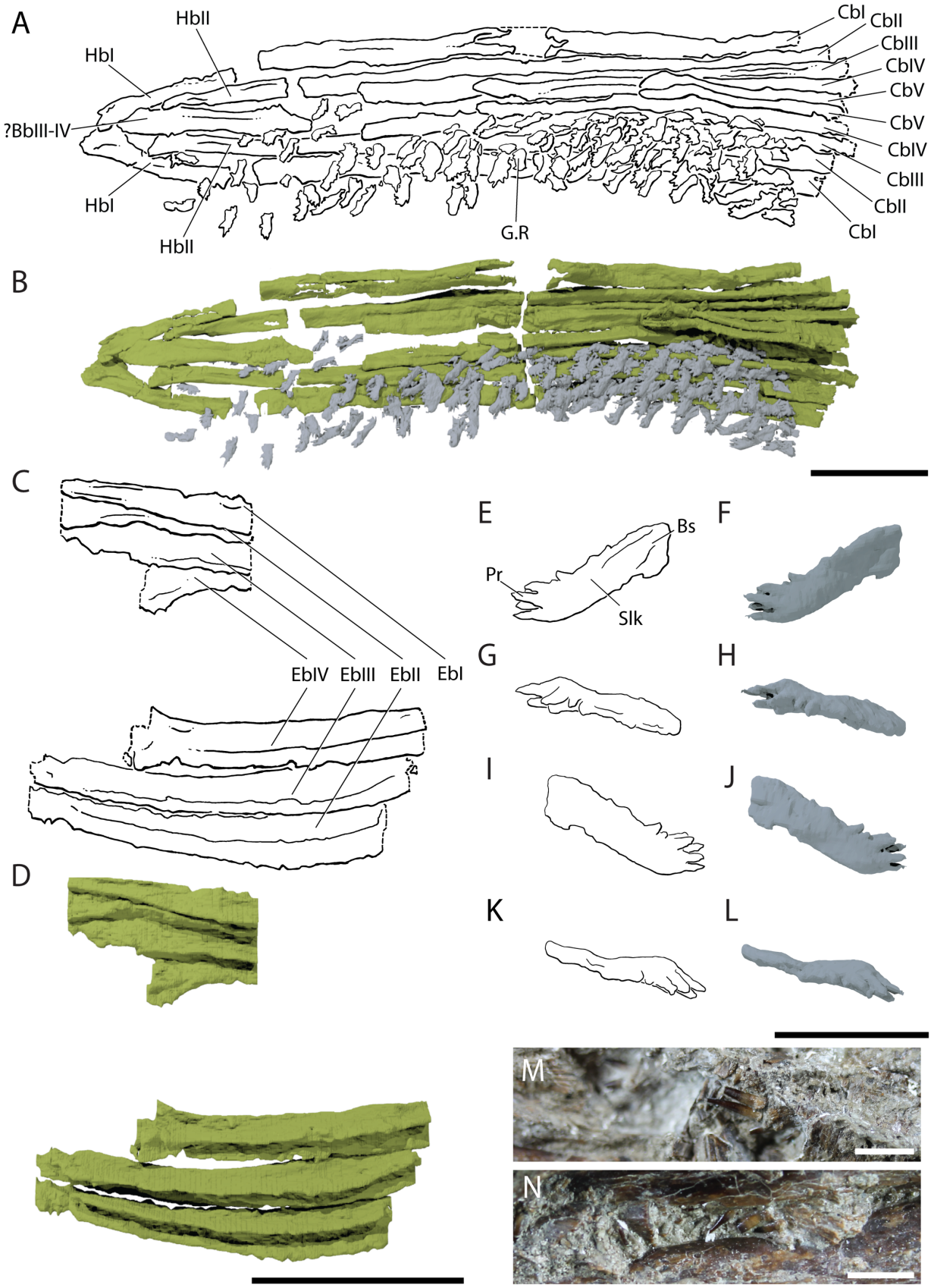

FIG. 7. Dorsal and ventral gill skeleton and associated rakers of *Martillichthys renwickae* NHMUK PV P.61563P. A, interpretive line drawing of ventral gill skeleton in dorsal view. B, three-dimensional rendering of ventral gill skeleton in dorsal view. C, interpretive line drawing of dorsal gill skeleton in dorsal view. D,

three-dimensional rendering of dorsal gill skeleton in dorsal view. E, interpretive line drawing of raker in dorsal view. F, three-dimensional rendering of raker in dorsal view. G, interpretive line drawing of raker in anterodorsal view. H, three-dimensional rendering of raker in anterodorsal view I, interpretive line drawing of raker in ventral view. J, three-dimensional rendering of raker in ventral view.. K, interpretive line drawing of raker in anteroventral view. L, three-dimensional rendering of raker in anteroventral view. M, photograph of gill raker teeth in dorsal view. N, photograph of gill raker teeth in dorsal view. Anterior to the left in panels A–F. Dashed lines indicate areas where margins are uncertain. *Abbreviations*: ?Bb, basibranchial; Bs, base; Cb, ceratobranchial; Eb, epibranchial; Hb, hypobranchial; G.R, gill raker; Pr, projections; Slk, stalk. Scale bars for panels A–D represent 5 cm, 2 cm for panels E–L and 0.5 cm for panels M-N. *(intended for full page width)*

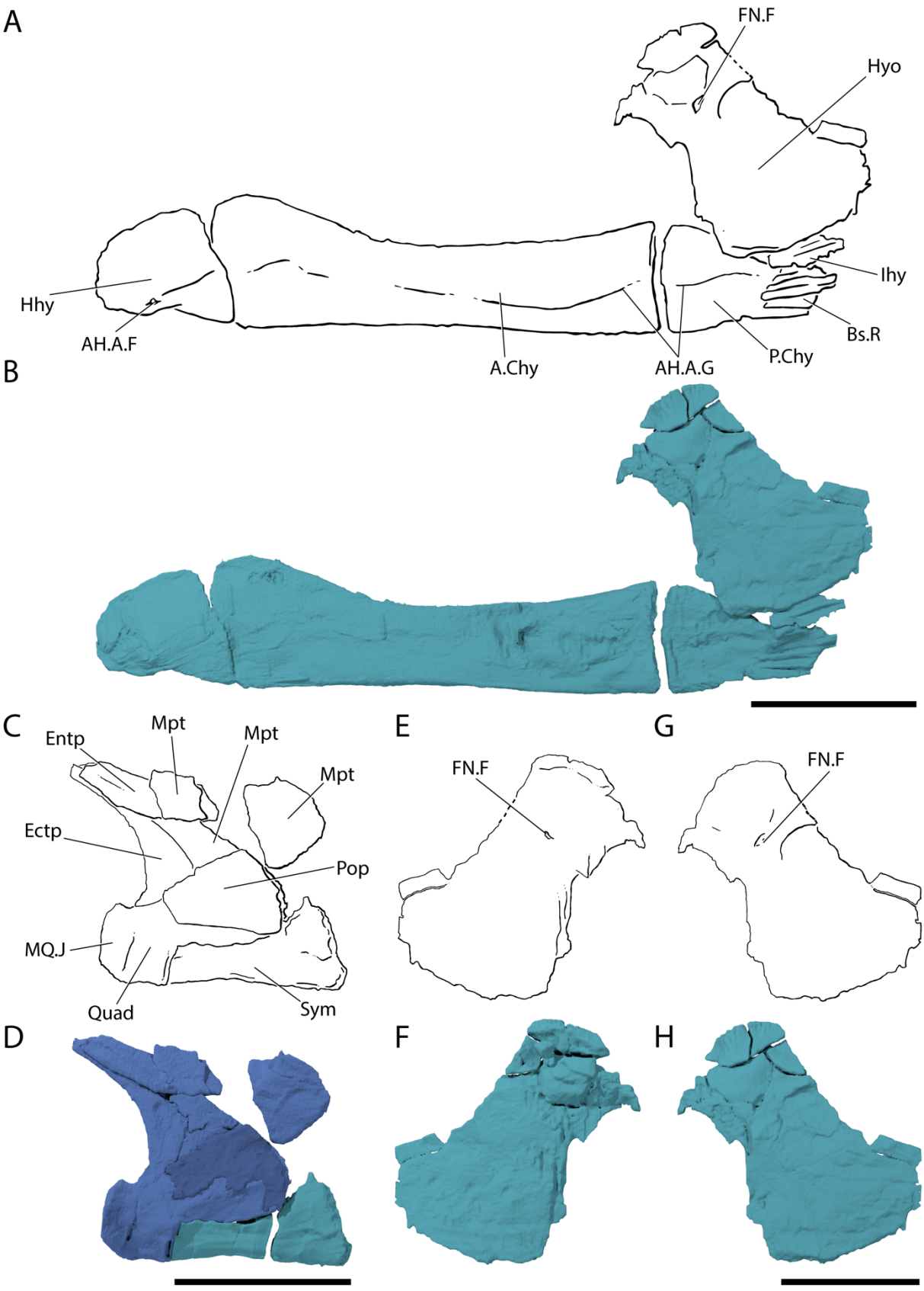

FIG. 8. Hyoid arch and palate of *Martillichthys renwickae* NHMUK PV P.61563P. A, interpretive line drawing of the left hyoid arch in lateral view. B, three-dimensional rendering of the left hyoid arch in lateral view. C, interpretive line drawing of the left palate in lateral view. D, three-dimensional rendering of the left

palate in lateral view. E, interpretive drawing of the left hyomandibula in mesial view. F, three-dimensional render of the left hyomandibula in mesial view. G, interpretive drawing of the left hyomandibula in lateral view. H, three-dimensional render of the left hyomandibula in lateral view. Anterior to the left in panels A–D, G and H; to the right in panels E and F. Dashed lines indicate areas where margins are uncertain. *Abbreviations*: A.Chy, anterior ceratohyal; AH.A.F, afferent hyoid artery foramen; AH.A.G, afferent hyoid artery groove; Bs.R, branchiostegal rays; Ectp, ectopterygoid; Entp, entopterygoid; FN.F, hyomandibular branch of the facial nerve foramen; Hhy, hypohyal; Hyo, hyomandibula; Ihy, interhyal; Mpt, metapterygoid; MQ.J, mandibular-quadrate joint; P.Chy, posterior ceratohyal; Pop, preoperculum; Quad, quadrate; Sym, symplectic. Scale bars represent 5 cm. *(intended for full page width)*

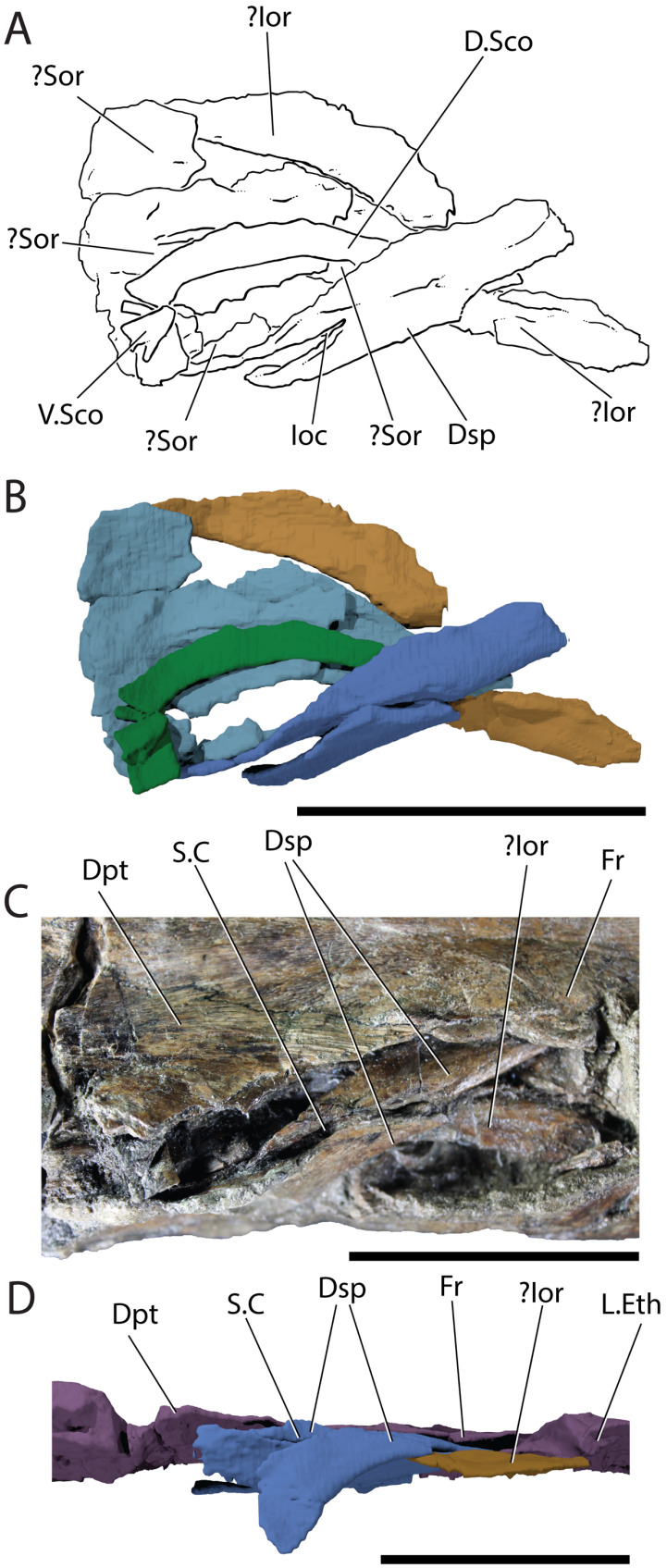

FIG. 9. Sclerotic ossicle and circumorbital bones of *Martillichthys renwickae* NHMUK PV P.61563P. A, interpretive drawing of right orbital region in dorsal view. B, three-dimensional render of right orbital region in dorsal view. C, photograph of right orbital region in dorsal view. D, three-dimensional render of right

orbital region in lateral view. Anterior to the right. *Abbreviations*: D.Sco, dorsal sclerotic ossicle; Dsp, dermosphenotic; Dpt, dermopterotic; Fr, frontal; ?Ior, infraorbital; L.Eth, lateral ethmoid; S.C, sensory canal; ?Sor, suborbital; V.Sco, ventral sclerotic ossicle. Scale bar represents 5 cm. *(intended for column width)*

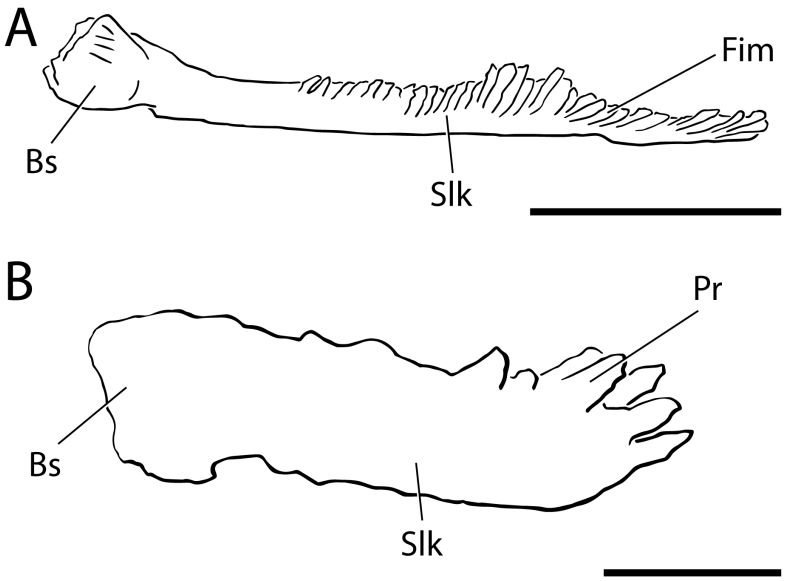

FIG. 10. Comparative gill-raker morphology of *Leedsichthys* and *Martillichthys*. A, interpretive drawing of gill rakers found in *Leedsichthys* (modified from Liston 2013, Fig. 1F; NHMUK P.6921) in lateral view. B, interpretive drawing of gill rakers found in *Martillichthys*, NHMUK PV P.61563P. *Abbreviations*: Bs; base; Fim, fimbriations; Pr, elongate, pointed projections, Slk, stalk. Scale bars represent 1 cm. *(intended for column width)*

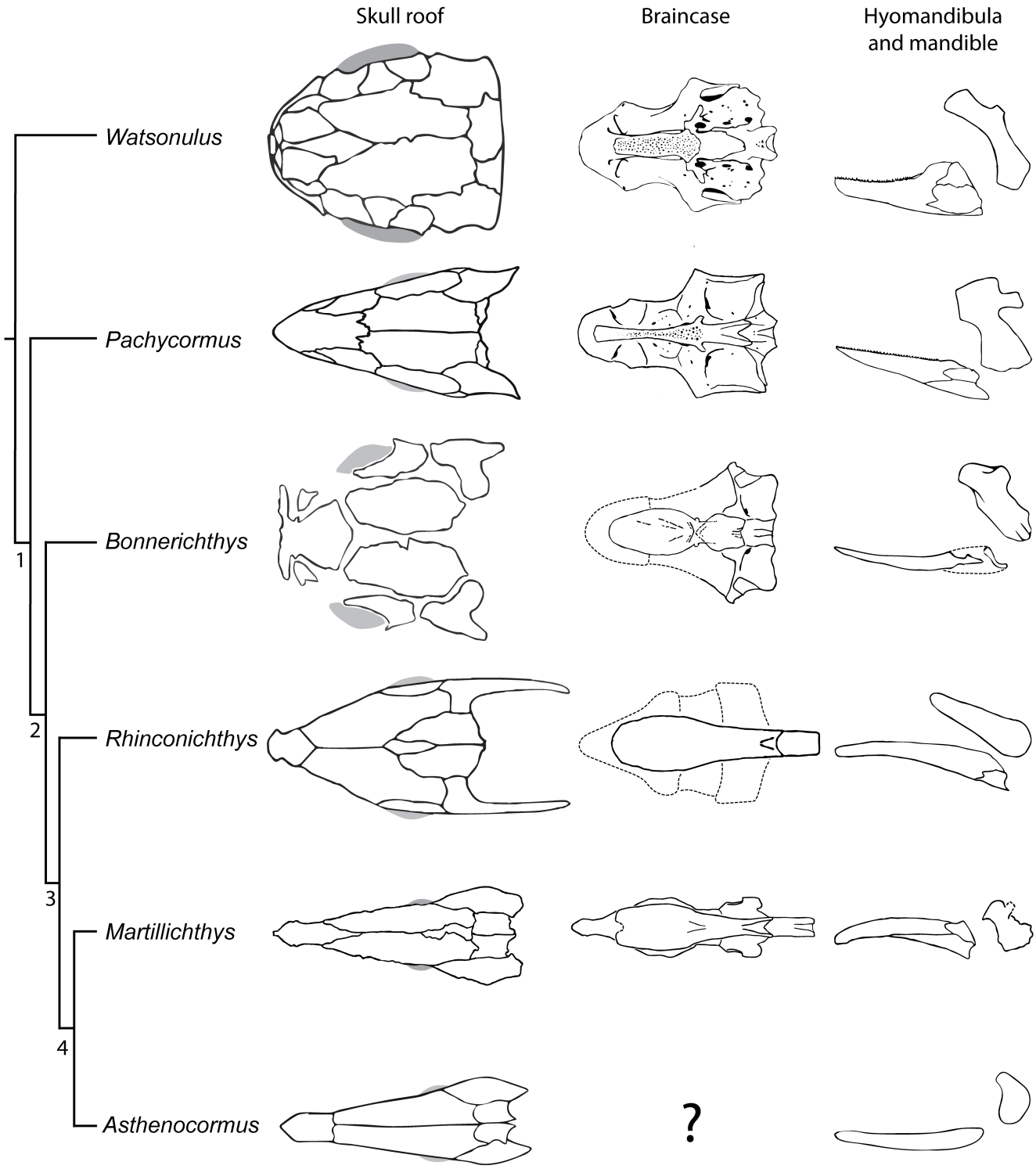

FIG. 11. Hand-drawn cladogram showing pachycormiform relationships, with comparisons of major aspects of cranial anatomy. Relationships based on Friedman (2012*a*) and argumentation given in text. Stippling on the parasphenoid indicates extent of the denticle field, if present. Shading indicates placement of eyes. Dashed lines indicate areas where margins are uncertain. Node 1: compound rostrodermethmoid; reduced coronoid process; absence of supraorbitals; elongate pectoral fins; bifurcating, asymmetrical, lepidotrichia. Node 2: absence of marginal dentition; lack of ornamentation on skull bones; absence of a supramaxilla;

broad anterior corpus of parasphenoid; posterior margin of parietals form median projection; absence of skull roof posterior boss; reduction/loss of scales; reduction/loss of caudal fin segmentation; gap between frontals. Node 3: elongated occipital stalk; elongated, ornamented gill rakers. Node 4: waisted hyomandibula; highly reduced posterior dermopterotic process; elongated pre-orbital region; and a short hyomandibula. *Asthenocormus* redrawn from Lambers (1992); *Bonnerichthys* redrawn from Friedman *et al.* (2010); *Pachycormus* redrawn from Lehman (1949) and Mainwaring (1978); *Rhinconichthys* redrawn from Friedman *et al.* (2010) and Schumacher *et al.* (2016); *Watsonulus* redrawn from Olsen (1984). *(intended for full page width)*